1. Report No.	2. Government Accession No.	3. Recipient's Catalog No.

4. Title and Subtitle	5. Report Date
A Data-driven Framework for Damage Diagnosis of Coastal Bridges	**June 2017**
	6. Performing Organization Code
7. Author(s) **Chao Sun, Ph.D.** **Zhiming Zhang**	8. Performing Organization Report No.
9. Performing Organization Name and Address **Department of Civil and Environmental Engineering** **Louisiana State University** **Baton Rouge, LA 70803**	10. Work Unit No.
	11. Contract or Grant No. **LTRC Project Number: 17-4TIRE** **State Project Number: DOTLT1000138**
12. Sponsoring Agency Name and Address **Louisiana Department of Transportation and Development** **P.O. Box 94245** **Baton Rouge, LA 70804-9245**	13. Type of Report and Period Covered **Final Report** **July 2016 – June 2017**
	14. Sponsoring Agency Code

15. Supplementary Notes

Conducted in Cooperation with the U.S. Department of Transportation, Federal Highway Administration

16. Abstract

Coastal bridges are exposed to multiple hazardous conditions including the corrosive environment, strong winds, storm surges and waves, abutment scour, possible vessel collisions and so forth. All these factors deteriorate the bridges, reduce their load-carrying capacities and even cause the bridges to collapse. A well-known catastrophic example is the I-35 Bridge that collapsed in Minneapolis during the summer of 2007. Therefore, accurate integrity evaluation and damage diagnosis of bridges will significantly enhance public safety and the nation's economic development.

This research project proposes a novel data-driven framework to implement damage diagnosis (damage localization and quantification) for coastal bridges. Pattern recognition through supervised machine learning methods is conducted to identify the damage. Different machine learning methods have been tried and evaluated. The Artificial Neural Networks (ANNs) approach has been demonstrated accurate and efficient and thus adopted in the framework. To reduce the computational cost, a two-step diagnosis strategy is used in the framework where damage localization is conducted in the first step through classification and damage quantification is carried out in the second step through classification\regression. Damage sensitive features including the normalized modal frequencies variation, mode shapes variation and modal curvatures are extracted to train the model. The established framework was examined on a Finite Element (FE) model of a 3-span reinforced concrete bridge. It is found that single/multiple damage location presence in the bridge girder and the pier can be detected and quantified with high accuracy. In addition, bridge scour can also be quantified well.

17. Key Words	18. Distribution Statement
damage dianosis; supervised machine learning; artificial neural networks; feature extraction; multiple degrees of freedom system; bridge damage; multi-label classification	**Unrestricted. This document is available through the National Technical Information Service, Springfield, VA 21161**

19. Security Classification (of this report)	20. Security Classification (of this page)	21. No. of Pages	22. Price
N/A	**N/A**	**74**	**N/A**

Project Review Committee

Each research project will have an advisory committee appointed by the LTRC Director. The Project Review Committee is responsible for assisting the LTRC Administrator or Manager in the development of acceptable research problem statements, requests for proposals, review of research proposals, oversight of approved research projects, and implementation of findings.

LTRC appreciates the dedication of the following Project Review Committee Members in guiding this research study to fruition.

LTRC Administrator/ Manager

Vijaya Gopu, Ph.D., P.E.
Professor

Members

Directorate Implementation Sponsor

A DATA-DRIVEN FRAMEWORK FOR DAMAGE DIAGNOSIS OF COASTAL BRIDGES

by

Chao Sun, Ph.D.
Assistant Professor

Zhiming Zhang, Ph.D. Candidate,
Research Assistant

Department of Civil and Environmental Engineering
M3316 Patrick F. Taylor Hall
Louisiana State University
Baton Rouge, LA 70803

LTRC Project No. [17-4TIRE]
State Project No. [DOTLT1000138]

conducted for

Louisiana Department of Transportation and Development
Louisiana Transportation Research Center

June 2017

ABSTRACT

Coastal bridges are exposed to multiple hazardous conditions including the corrosive environment, strong winds, storm surges and waves, abutment scour, possible vessel collisions and so forth. All these factors deteriorate the bridges, reduce their load-carrying capacities and even cause the bridges to collapse. A well-known catastrophic example is the I-35 Bridge that collapsed in Minneapolis during the summer of 2007. Therefore, accurate integrity evaluation and damage diagnosis of bridges will significantly enhance public safety and the nation's economic development.

This research project proposes a novel data-driven framework to implement damage diagnosis (damage localization and quantification) for coastal bridges. Pattern recognition through supervised machine learning methods is conducted to identify the damage. Different machine learning methods have been tried and evaluated. The Artificial Neural Networks (ANNs) approach has been demonstrated accurate and efficient and thus adopted in the framework. To reduce the computational cost, a two-step diagnosis strategy is used in the framework where damage localization is conducted in the first step through classification and damage quantification is carried out in the second step through classification\regression. Damage sensitive features including the normalized modal frequencies variation, mode shapes variation and modal curvatures are extracted to train the model. The established framework was examined on a Finite Element (FE) model of a 3-span reinforced concrete bridge. It is found that single/multiple damage location presence in the bridge girder and the pier can be detected and quantified with high accuracy. In addition, bridge scour can also be quantified well.

ACKNOWLEDGMENTS

This research was funded by the Transportation Innovation for Research Exploration (TIRE) program of Louisiana Transportation and Research Center (LTRC). The principal investigator (PI) would like to thank LTRC for providing him the opportunity to explore this novel idea for damage diagnosis. The PI would like to acknowledge Dr. Vijaya Gopu, P.E., from LTRC for his support of this exploratory research. Without his support, this project would not have been completed. During the project, Dr. Mingxuan Sun and Changbin Li from the Division of Computer Science and Engineering at Louisiana State University provided substantial help to apply the machine learning methods. Their help is also greatly acknowledged.

Any opinions, findings, conclusions, or recommendations expressed in this material are those of the authors and do not necessarily reflect the views of the sponsoring agencies.

IMPLEMENTATION STATEMENT

The research conducted in this project is exploratory in nature. The PI's idea to establish a data-driven framework for structural health monitoring has been investigated and verified. Results indicated that pattern recognition through the supervised machine learning methods can localize and quantify the structural damage efficiently and accurately. In addition to its application to bridges, the verified approach can be potentially applied to a large range of engineering structures for damage diagnosis.

Since the presented work is essentially numerical study, further experimental research will be implemented through lab tests. As the outcomes of the project, two journal papers based on the research results are being prepared and will be submitted soon. Structural condition monitoring actually consists of two steps: damage diagnosis and damage prognosis. The presented research is essentially the first step for damage prognosis where the focus is to evaluate the structural security and predict the remaining useful life. As the first step of the PI's research plan, the obtained results from this project will be incorporated as the preliminary results in a more comprehensive proposal which is under development.

TABLE OF CONTENTS

LIST OF TABLES

LIST OF FIGURES

INTRODUCTION

A large number of bridges in Louisiana and the United States are working in coastal areas with multiple hazardous effects causing cumulative damage to bridges. To preserve the structural integrity and security, it is required that bridges in the United States be inspected and rated every two years. Currently, this is implemented using visual inspection techniques largely. The procedure however is slow and not quantifiable. In addition, the approach cannot provide visual data for inaccessible portions of bridges. Hence, it is possible that there will be damage going undetected during an inspection, which might cause bridge to collapse when the undetected damage on load-carrying members is beyond the critical level. A well-known catastrophic example is the I-35 Bridge that collapsed in Minneapolis during the summer of 2007, see Figure 1.

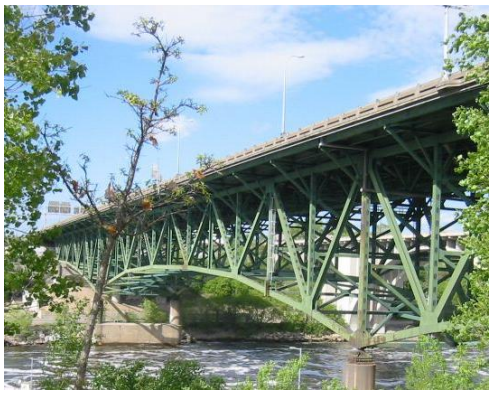

(a) Before collapse

(b) After collapse

Figure 1
Minneapolis I-35W bridge before and after collapse

(Source: https://en.wikipedia.org/wiki/I-35W_Mississippi_River_bridge)

To overcome the drawbacks of the traditional visual inspection methodology, quantifiable and continuous approaches to bridge damage monitoring have been proposed and studied by researchers in the community of structural health monitoring (SHM). Basically, the SHM can be implemented using a model- or a data-based approach [1]. Model-based approaches are commonly based on a Finite Element (FE) model representing the structure of interest. The basic idea is that once an initial FE model is created, measured data from the real structure is used to update the structural matrices (mass, stiffness and damping) such that the updated model can more accurately represent the real structure. Based on the updated model, damage detection, localization and quantification can be conducted through solving an inverse problem using measured data from the structure under test. This method has attracted a great deal of effort in research and demonstrated effective for damage identification [2, 3]. However, the model-based method is challenged by the fact that the inverse problem is often ill-posed and requires careful regularization [4, 5]. In addition, this method is susceptible to

the uncertainty of the measurements and the structures.

As an alternative, the data-based approach which is statistical in nature implements the diagnosis of SHM through pattern recognition rather than the physics law of the model. Machine learning algorithms are well developed to implement the pattern recognition. The learning process is to establish the relationship between some features and the damaged state of the structure [1]. Learning naturally falls into two categories: unsupervised learning and supervised learning. Unsupervised learning refers to the case where the training data is not labelled and only the intrinsic relationships within the data can be learnt. Supervised learning refers to the case where the training data is acquired from multiple classes and labels for the classes are known. While implementing this approach, the possible damage states are labelled and associated with the features extracted from the measured data. In comparison with the model-based approaches, data-based approaches can avoid the issues due to reverse modelling in the model-based approaches. Further, uncertainty of the measured data and the structures is automatically accommodated.

While the data-based approaches are advantageous over the model-based approaches in many aspect, the lack of data from the structures in both undamaged and damaged states, especially data from large-scale and high value structures, challenges the application of this approach. To address this limitation, the present research project explored the idea to integrate the model-updating technique with the data based approach. The basic idea is to have an accurate updated FE model. Data from damaged and undamaged states of the structure can be generated numerically to train the machine learning algorithm. Since the mode is updated, the numerical data can be regarded to be reliable for training purses.

OBJECTIVE

The objective of this study is to investigate the data-based approaches for damage diagnosis of bridges and other structures. The proposed new approach is different from other approaches that have been reported in the literature. In the proposed approach, numerical models generate massive data corresponding to undamaged and damaged states for training. Different machine learning methods have been tested and the artificial neural networks (ANNs) approach is finally selected and demonstrated to be accurate and efficient.

SCOPE

The proposed data-driven approach for damage diagnosis of bridges has the potential to be applied to a large range of structural and mechanical structures. Examples of such applications include high rise buildings, energy infrastructures, aerospace structures and so forth. The research conducted in this project is primarily focused on numerical study which will be extended and verified in the next step. In this study, only the ANNs classification and regression method is used for damage localization and quantification. In fact, other machine learning methods, like reinforcement learning, deep learning and other approaches are expected to perform similarly well or better. This will be investigated in the next step of the research.

LITERATURE REVIEW

The general data-based approach for damage diagnosis can be implemented through four procedures [1]: (1) operational evaluation, (2) data acquisition, (3) feature selection and (4) pattern recognition for feature discrimination. Since the present project focuses on (3) and (4), a brief literature review is presented here regarding feature extraction and pattern recognition.

Feature Extraction for SHM

To efficiently locate and quantify the structural damage through pattern recognition, extraction of a damage-sensitive feature which is some quantity that can be used to indicate damage is of critical important. Identifying features that can accurately distinguish a damaged structure from an undamaged one is the primary topic of SHM [6]. If good features are selected, the pattern recognition for damage diagnosis can be performed accurately and quickly. Otherwise, the process becomes inefficient. The following subsections will present a review on some appropriate features.

Modal property features

Damage localization and quantification on the basis of vibration signals has been developed for many years [7-11].

Initially, researchers tried to use measured natural frequencies for damage localization since the technique was not good enough to identify the mode shapes with acceptable accuracy. However, this approach is limited because that the information provided by natural frequencies is insufficient and it is possible that the damage is located incorrectly when just using natural frequencies. For symmetrical structures, damage at symmetric locations can't be differentiated since the changes in natural frequency are exactly the same.

As mode shape measurement technique advances, many researchers have exerted their efforts to the area of damage detection using mode shape information [12-14]. It was proved that the ratio of frequency changes in two modes due to localized damage is only a function of the damage location and not the damage extent [15]. In addition, the normalized frequency change ratio (NFCR) was also a function only of the damage location [16]. The fractional frequency change (FFC) for the i^{th} mode is expressed as

$$\mathrm{FFC}_i = \frac{f_{ui} - f_{di}}{f_{ui}} \tag{1}$$

where f_{ui} and f_{di} are the frequencies of the i^{th} mode of the structure in undamaged and damaged states respectively.

The NFCR for the i^{th} mode is defined as:

$$\mathrm{NFCR}_i = \frac{\mathrm{FFC}_i}{\sum_{j=1}^{p} \mathrm{FFC}_j} \tag{2}$$

where p is the number of modes with measured natural frequencies.

It is worth to note that all the above parameters are derived from natural frequencies and therefore cannot discriminate between two symmetric damage locations. A combined damage signature index (DSI) consisting of both mode shapes and frequencies were proposed in [17]. It was found that the index DSI depends on damage location only, not on extent. The DSI is defined as the ratio of change in modal vector to change in modal eigenvalue, namely,

$$\boldsymbol{DSI}_i = \frac{\{\boldsymbol{\Phi}_{ui}\} - \{\boldsymbol{\Phi}_{di}\}}{f_{ui}^2 - f_{di}^2} \tag{3}$$

where $\{\boldsymbol{\Phi}_{ui}\}$ and $\{\boldsymbol{\Phi}_{di}\}$ are the modal vector values of the i^{th} mode in undamaged and damaged states respectively. They can be incomplete. When only a few modal vector values at K locations are obtained, the vector $\boldsymbol{DSI}_i$ comprises K entries. If only one modal value is available, $\boldsymbol{DSI}_i$ reduces to a scalar quantity.

Transmissibility function features

Chen *et al.* first proposed transmissibility function as a feature for damage detection in 1994 [18], since when the transmissibility function has been widely used for structural damage detection and characterization [19-20]. Experimental studies validated the efficiency of transmissibility function for damage detection [21-23] and localization [24]

Damage detection taking transmissibility function as the features mainly use three novelty detection methods, i.e., auto-associative neural networks, outlier analysis, and kernel density estimation; while damage localization primarily uses the artificial neural network (ANN). In addition to its high sensitivity to damage, the transmissibility function necessitates no measure of the excitation.

Transmissibility function is obtained by taking the ratio of the system's input spectra and output spectra:

$$T_{ij}^k(\omega) = \frac{x_i^k(\omega)}{x_j^k(\omega)} = \frac{(-1)^{k+i} \det\left(\left[K - \omega^2 M\right]\right)_{ik}}{(-1)^{k+j} \det\left(\left[K - \omega^2 M\right]\right)_{jk}} \tag{4}$$

Modal curvature features

Pandey *et al.* [25] for the first time proposed to use the modal curvature for damage detection. The modal curvature can be calculated using Eq. (5).

$$v'' = \frac{(v_{i+1} - 2v_i + v_{i-1})}{h^2} \tag{5}$$

Where v_i is the mode shape amplitude at the i^{th} point; h is the distance between two successive measured locations.

Abdel *et al.* [26] used the modal curvature to detect bridge damage and obtained promising results. However, modal curvature works well for lower mode shape while higher modal curvature might produce false damage indication. Therefore, the low modal curvatures are good features for damage identification.

Pattern Recognition for Damage Diagnosis

Pattern recognition for damage diagnosis is to apply an algorithm to decide the damage state on the basis of the given feature input. Two basic types of algorithm can be used for this purpose in a supervised learning manner: classification and regression.

Multi-class classification

Multi-class classification has been widely used for damage detection and localization by taking the damage condition and damage location combinations as the target categories for classification. Multi-class classification treats the cases with multiple damage locations as exclusive category labels. This approach of labelling omits the interconnection between two damage cases that contain common damage locations. For example, the case with damage locations A, B, and C and that with A and B must share common characteristics that help detection the common damage locations (A and B) and discern the distinct location (C). As will be demonstrated in the examples below, neglecting the relation between damage cases, multi-label classification necessitates more instances to obtain an acceptable accuracy, and thus has lower damage detection efficiency.

Binary classification

Binary classification classifies the elements of a given set into two groups using a classification rule. Binary classification can be used for damage detection on the structural scale or with respect to a certain location on a structure, by making a decision about whether a structure possesses certain properties or characteristics. Binary classification reduces the multi-label classification problem as it decomposes the classification task into multiple independent problems with binary classification labels [27-28].

For damage detection and localization, binary classification trains all the instances for each possible damage location separately setting the damage condition at that location (damaged or not) as the target label, and finally integrates the classification results for all the damage locations to formulate a model for multi-label classification decision making. However,

binary classification, by separating classes with multiple labels, fail to take into account the correlation between the instance's labels and weakens the system's expressive power. [29]

Multi-label classification

Multi-label classification problems widely exist in the real world problem solutions. For instance, a movie may possess the characteristics labelling it into more than one categories, such as western and action. The multi-label learning problem represented each example an instance with a set of labels, aims at generating a label set that categorize the example with an acceptable accuracy.

Intuitively, multi-label learning deals with ambiguous objects possessing multiple semantic meanings simultaneously. Zhang and Zhou proposed the InsDif (instance differentiation) method to solve the multi-label learning problem by considering the ambiguity of objects in the input space (instance space) [30]

It is assumed that an object belongs to several semantic classes simultaneously due to the diverse information contained in the object. This method represents the ambiguous objects using a bag of instances instead of a single instance, where each instance in the bag explicitly reflects some information contained in the object from a certain aspect and produces more effective solution to the multi-label classification problem.

Regression

Regression used in this study refers to the statistic regression using machine learning method to quantify the damage severity at all the possible damage locations. The target is a vector containing the damage extents. This method necessitates high computational capacity, though it fulfills the objectives of damage detection, damage localization, and damage quantification using one operation of regression analysis.

METHODOLOGY

On basis of the literature review, the traditional machine learning methods including the support vector machine (SVM), the logistic regression (LR) and the artificial neural networks (ANNs) (as shown in Figure 2) are tested first and then the ANNs method will be selected to implement the pattern recognition. To reduce the computational cost, a two-step strategy of damage diagnosis is proposed. In the first step, training data are generated from all the possible combination of different damage locations. Here the number of damages considered are 1, 2 and 3. Once the number and locations of the damage is determined in the first step, a second pattern recognition/regression is conducted to quantify each of the damage in step 2. This two-step strategy is illustrated in Figure 3

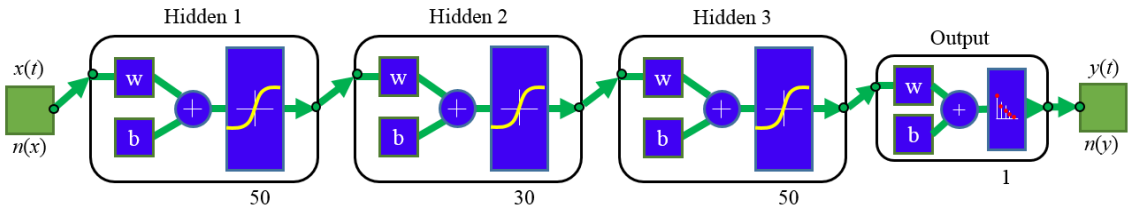

Figure 2
Neural network configuration

The proposed machine learning framework for damage diagnosis is first tested on an 8 degrees-of-freedom (8DOF) lumped mass system representing a simplified structural or mechanical system. Then a real bridge model of a 3-span reinforced concrete bridge is used to examine the efficiency and accuracy of the proposed framework. Detailed procedures and results with respect to the two scenarios are presented next.

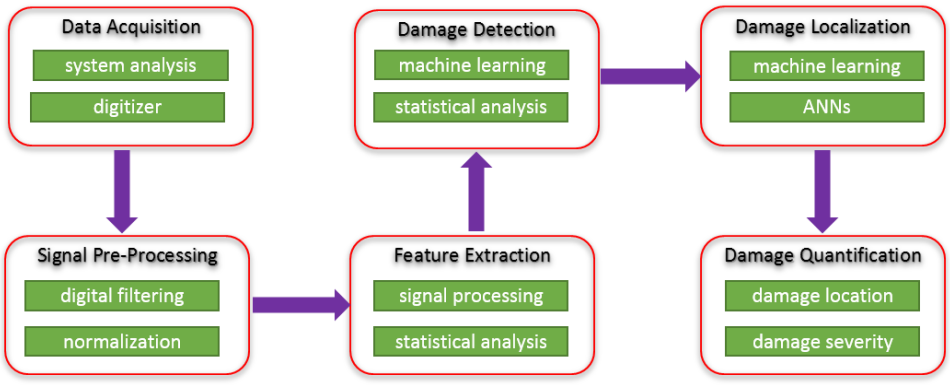

Figure 3
Flowchart of the data-driven damage diagnosis framework

RESULTS AND DISCUSSIONS

Damage diagnosis of an eight DOF lumped mass system

Model description

This section performs damage diagnosis with respect to a generic structure represented by an 8-DOF system containing eight lumped masses, nine connecting springs, and nine connecting dampers, as shown in Figure 4. Table 1 lists the non-dimensional values of the masses, spring, and damping coefficients that are assigned to the model.

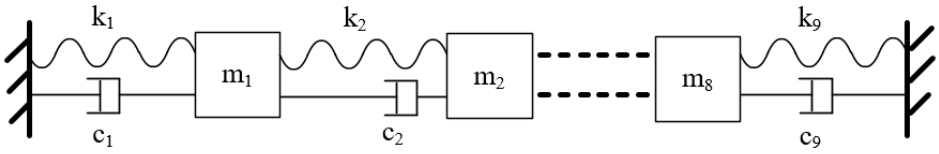

Figure 4
Configuration of the eight-DOF lumped mass system

Table 1
Mechanical properties of the eight-DOF model

Item	I	II	III	IV	V	VI	VII	VIII	IX
M	1	2	3	4	2	2	1	3	-
C	20	20	20	20	20	20	20	20	20
K	10000	10000	10000	10000	10000	10000	10000	10000	10000

A preliminary study

In the beginning, it is unclear about the selection of good damage-sensitive features, an appropriate learning method and suitable external loading conditions. Hence, a preliminary study is conducted for the 8-DOF system with selected damage severity and positions. Table 2 shows the damage conditions for this preliminary study

Table 2
Damage conditions indicated by spring stiffness reduction

Damage condition	Case 1	Case 2	Case 3
DC I	2% on k_1	10% on k_1	50% on k_1
DC II	2% on k_2	10% on k_2	50% on k_2
DC III	2% on k_3	10% on k_3	50% on k_3
DC IV	10% on k_1 and 50% on k_2		
DC V	10% on k_2 and 50% on k_3		

Three loading conditions, i.e. harmonic loading, impact loading and white noise excitations are utilized. The transmissibility function is initially extracted as the input feature. A total number of 18 cases are considered herein with different loading masses (LM) and masses for the transmissibility function calculation (TM1 and TM2). As an evaluation index, *Precision*, *Recall* and *F-score* are the primary parameters ranging from 0 to 1 often used to evaluate the accuracy of the algorithm. Detailed definition of the three parameters are not presented here. Generally the closer the parameter value is to 1, the more accurate predictions are provided.

Table 3 lists the identification result corresponding to the 18 cases as described above. In Table 3, the parameter minVal refers to the minimal value of the *Precision*, *Recall* and *F-score* calculated in each of the cases. The results indicate that the impact loading has best performance for damage identification, white noise excitation has intermediate performance and the harmonic loading has the least.

Figure 5 shows the confusion matrix of classification using support vector machines with a ten-fold cross validation. It shows that except Class 2, i.e., the first damage condition, all the instances belonging to other classes are classified right with al recall of 100%. The average recall is 97.65%; the average precision is 97.94%; the average f-score is 98.04%.

Figure 6 tabulates the confusion matrix of classification using logistic regression with a ten-fold cross validation. It shows that except Class 2, i.e., the first damage condition, all the instances belonging to other classes are classified right with al recall of 100%. The average recall is 95.07%; the average precision is 95.73%; the average f-score is 94.98%.

Figure 7 tabulates the confusion matrix of classification using neural networks with a ten-fold cross validation. It shows that except Class 2, i.e., the first damage condition, all the instances belonging to other classes are classified right with al recall of 100%. The average recall is 96.82%; the average precision is 97.30%; the average f-score is 97.95%.

Table 3
Results of damage localization in the preliminary study

ID	LM	TM1	TM2	minVal>0.7			minVal>0.8			minVal>0.9			minVal>0.95		
				H	I	W	H	I	W	H	I	W	H	I	W
1	1	1	2												
2	1	1	5												
3	1	1	8												
4	1	4	5												
5	1	4	8												
6	1	7	8												
7	4	1	2												
8	4	1	5												
9	4	1	8												
10	4	4	5												
11	4	4	8												
12	4	7	8												
13	7	1	2												
14	7	1	5												
15	7	1	8												
16	7	4	5												
17	7	4	8												
18	7	7	8												

Figure 5
Confusion matrix of classification using support vector machines

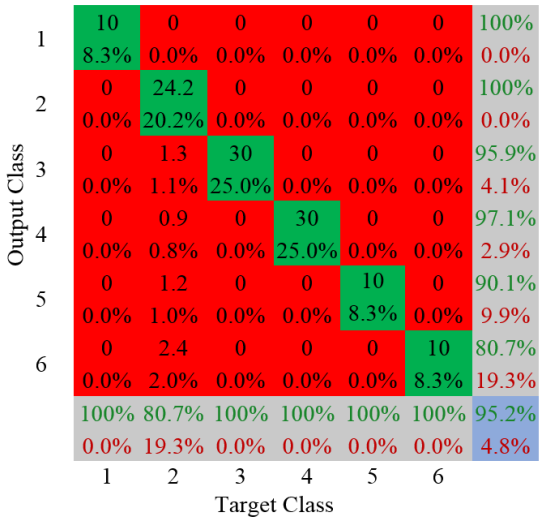

Figure 6
Confusion matrix of classification using logistic regression

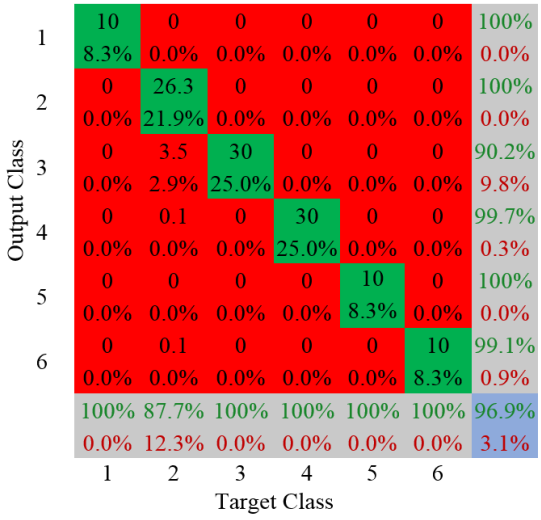

Figure 7
Confusion matrix of classification using neural networks

A general study

On the basis of the preliminary study, the neural networks method is selected as a primary learning method. Impact loading applied at the middle mass (mass 4 or mass 5) is adopted. As mentioned before, the scenarios corresponding to single damage, two damage and three damage are studied. Therefore, to consider all the possible combinations of different damage number and locations, a total number of 129 ($C_9^1 + C_9^2 + C_9^3$) classes are labelled and associated with the extracted damage-sensitive features.

Feature extraction

Damage is introduced through reducing the spring stiffness at the specific location. The

features used in this project include the normalized frequency and mode shape variations as defined in Eqns. (2) and (3). The input vector to the neural networks consists of combined modal parameters which is formulated as:

$$\{\text{Input}\} = \{\text{NFCR}_1\, \text{NFCR}_2 ... \text{NFCR}_m \times NDSI_1 NDSI_2 ... NDSI_n\} \tag{5}$$

where NFCRi (i = 1, 2,..., m) is the NFCR defined in Eq. (2), and NDSIi (i = 1, 2,…, n) is the normalized DSI defined as

$$NDSI_i(k) = \frac{DSI_i(k)}{\sum_{j=1}^{n} DSI_j(k)} \tag{6}$$

It is noted that the input vector defined in Eqn. (5) possesses the following attributes: (i) with the first-order approximation, the parameters of the input vector are only dependent on damage location and independent of damage extent; (ii) the input parameters can be derived using an arbitrary number of modal vector values, even with only one modal value available.

Dynamics modeling

Within each damage case, an impact load is applied to a specific mass (e.g. mass 5) and the free vibration response is processed using an out-put only method [33] to extract the modal frequencies and mode shapes. As an illustration, results of the single damage case are illustrated here and other results are presented in the Appendix.

Figure 8 shows the displacement of Mass 5 under the impact load under undamaged and damaged conditions. Figure 9 and Figure 10 show the decomposed modal response under damaged and undamaged conditions. One can see that the out-put only algorithm can satisfactorily decompose the response of mass 5 into each of the modes. Figure 11 and Figure 12 show the response spectrum under damaged and undamaged conditions. Figure 13 shows the comparison of the normalized mode shape between the undamaged and damaged cases. Table 4 lists the modal frequencies of the undamaged and damaged structure. One can find in Figure 13 and Table 4 that a single damage at spring 5 can cause significant variations of the natural frequency and the mode shapes.

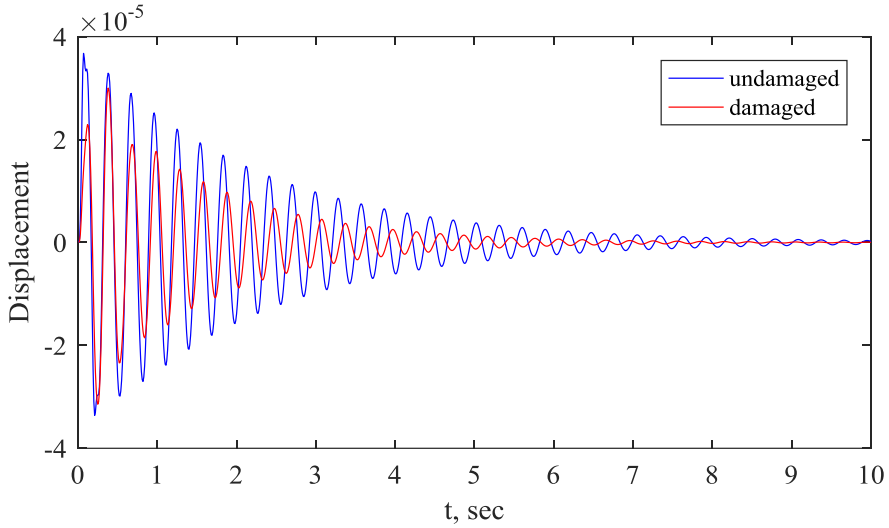

Figure 8
Displacement time history of mass 5 in undamaged and damaged conditions

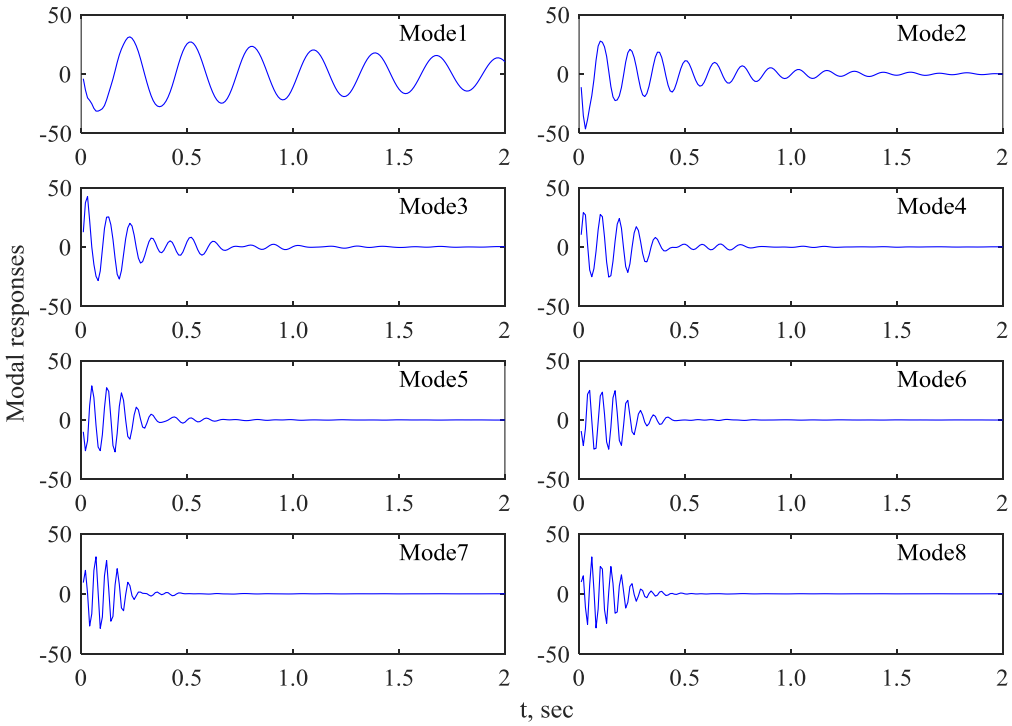

Figure 9
Modal responses of mass 5 in undamaged conditions

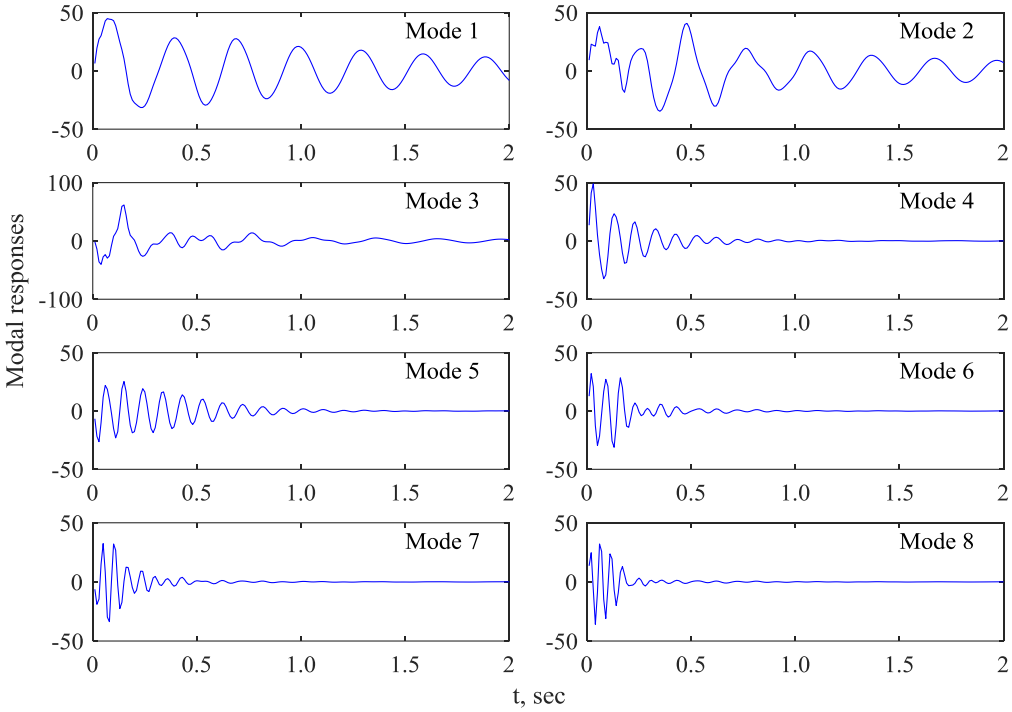

Figure 10
Modal responses in damaged conditions (single damage at spring 5)

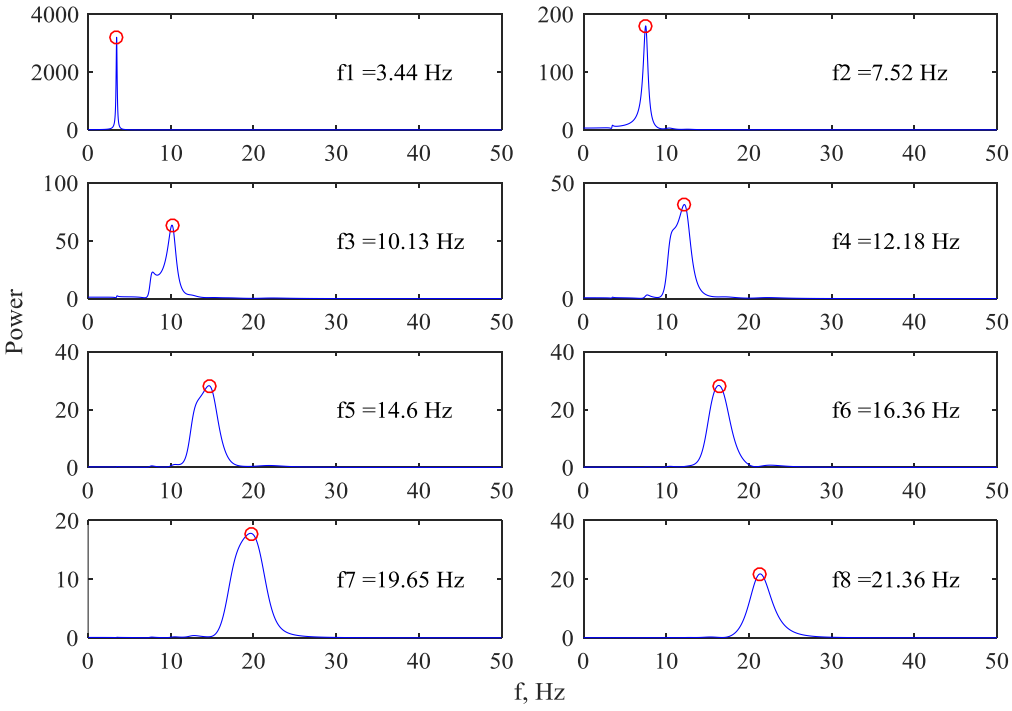

Figure 11
Modal response spectra in undamaged conditions

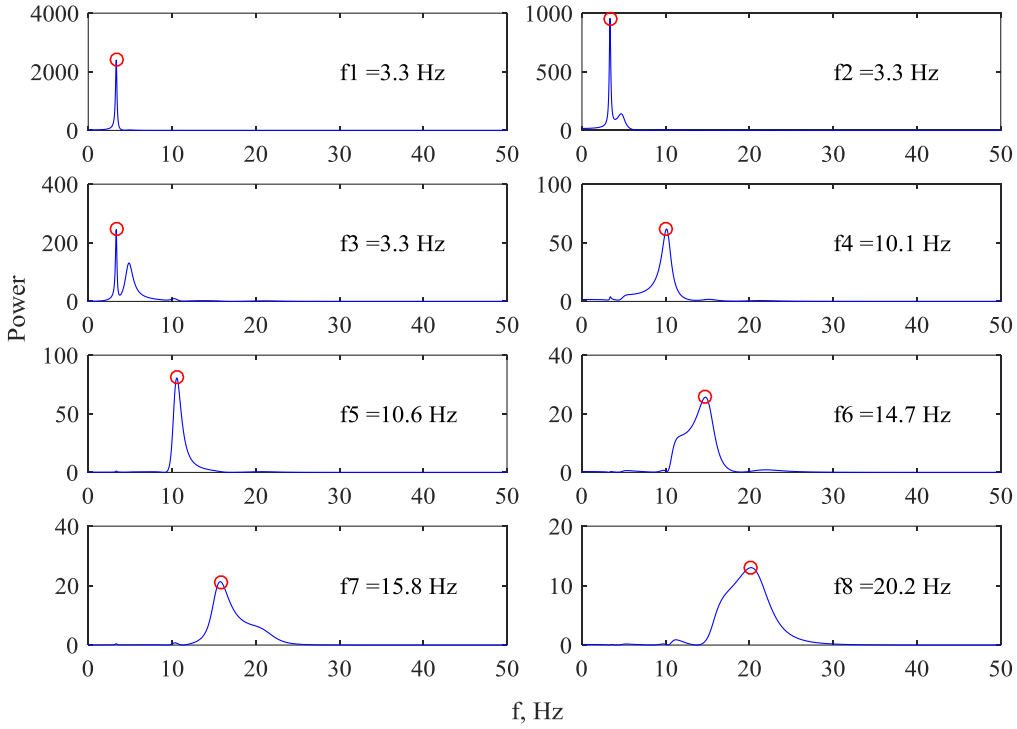

Figure 12
Modal response spectra in damaged conditions (single damage at spring 5)

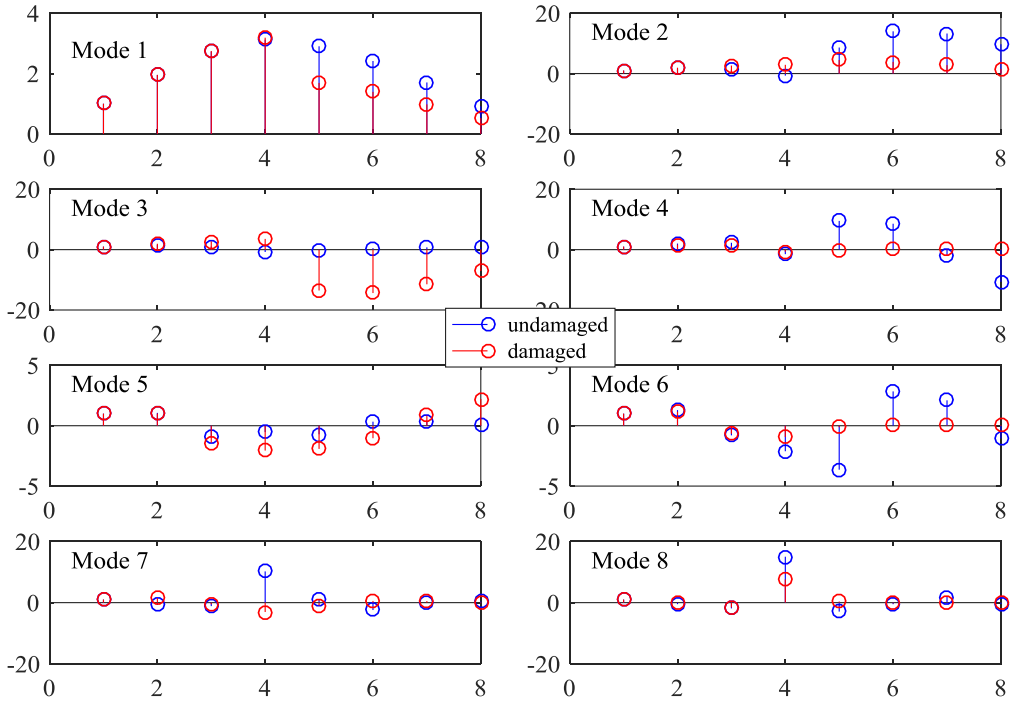

Figure 13
Normalized modal shape comparison between undamaged and damaged conditions

Table 4
Modal frequencies of undamaged and damaged systems (Unit: Hz)

Mode ID	1	2	3	4	5	6	7	8
undamaged	3.4	7.5	10.1	12.2	14.6	16.4	19.7	21.4
damaged	3.3	3.3	3.3	10.1	10.6	14.7	15.8	20.2

Patter recognition

The multi-class classification, binary classification and multi-label classification methods are evaluated here in this section.

Multi-class classification

Figure 14shows the classification result using the multi-class classification approach with 100 data points for each damage case. It can be seen that with 100 samples for each case, the classification results are satisfactory for the single damage case (class ID from 1 to 9). However, for around 20% of the damage cases, the identification result is not that satisfactory for a damage detection purpose, with many of the f-scores below 0.8.

In comparison, when the number of data points used to train the model increases to 1000, the classification results are improved significantly with most f-scores above 0.9 as shown in Figure 15

F-score of multi-class classification using 1000 data points for each class

.

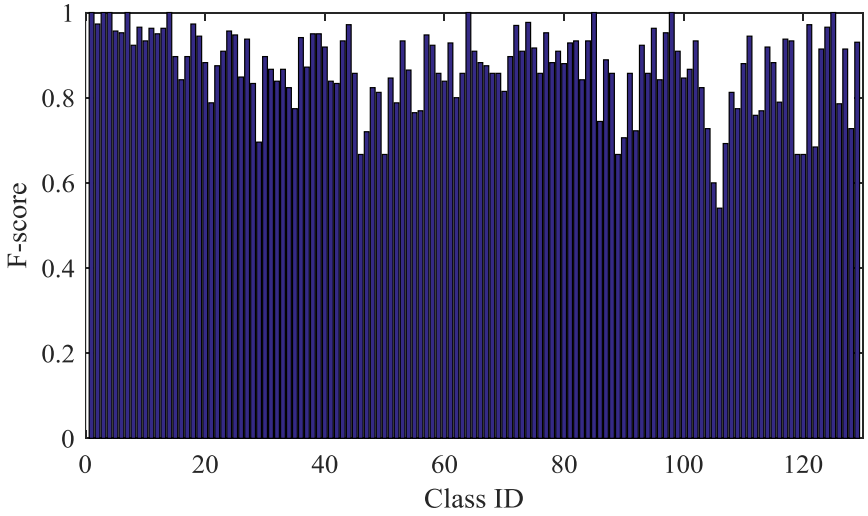

Figure 14
F-score of multi-class classification using 100 data points for each class

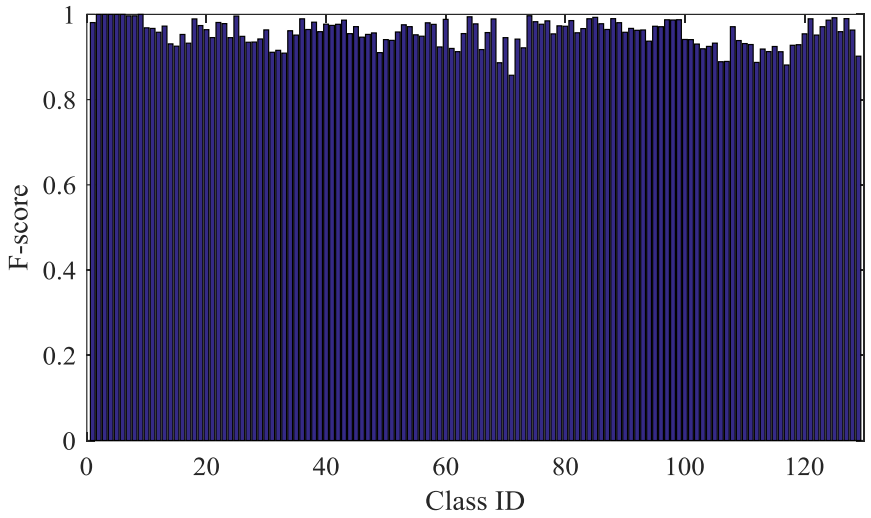

Figure 15
F-score of multi-class classification using 1000 data points for each class

Binary classification

As this numerical simulation considers the cases with at most three damage locations, most of the springs are not damaged in most cases. For example, the first spring is damage in 37 of the total 129 cases. As is expected, the binary classification has better classification results for the "No-damage" category for each location, which are demonstrated in Figure 16 and Figure 17.

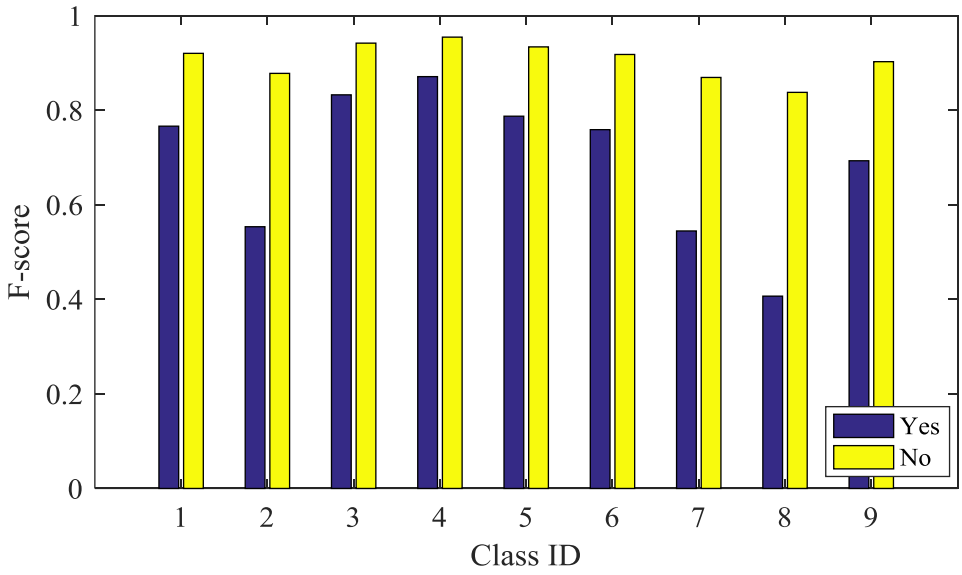

Figure 16
F-score of binary classification using 100 data points

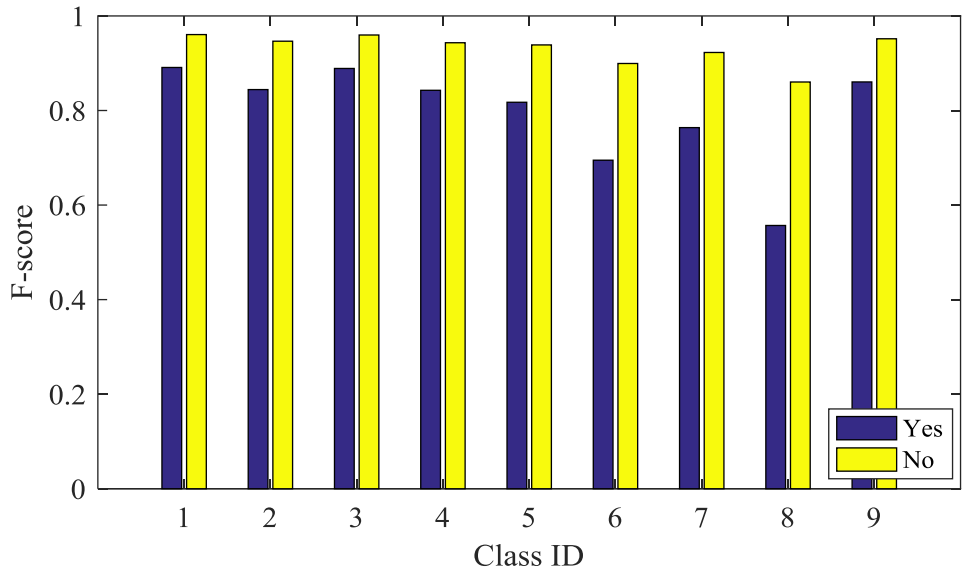

Figure 17
F-score of binary classification using 1000 data points

Multi-label classification

Table 5 and Table 6 illustrates the results of the multi-label classification using the instance differentiation method, and that from the integration of the binary classification results. In Table 5 and Table 6, Hamming loss is defined as the portion of instances having the output hypothesis different from the targets. One error evaluates how many times none of the predicted instance labels lies in the target class. The coverage measure denotes the average number of instances covering all the target labels. Average precision evaluates the average fraction of instance labels with the correct prediction. Ranking loss measures the average portion of instance labels that are ranked incorrectly [34].

It can be seen that with only 50 repeats the average precision can reach 0.9005 using multi-label classification, and that the multi-label classification results are much better than that of the binary classification.

Table 5
Results of multi-label classification using the instance differentiation method

Evaluation criterion	Number of repeats 10	30	50	100
Hamming loss	0.1606	0.1073	0.0939	0.0400
One-error	0.1163	0.0729	0.0504	0.1000
Coverage	3.3760	2.8031	2.6163	0.1000
Ranking loss	0.1445	0.0818	0.0604	0.0125
Average precision	0.8267	0.8818	0.9005	0.9500

Table 6
Integration of binary classification results

Evaluation criterion	Number of repeats 100	1000
Hamming loss	0.14	0.11
One-error	0.05	0.02
Coverage	3.76	3.44
Ranking loss	0.37	0.30
Average precision	0.81	0.85

Damage severity quantification

One damage location

Figure 18 and Figure 19 show the results of damage severity regression for the one-damage-location case using the neural networks method. This method applied a ten-fold cross validation to train the network and yield an average of the regression. Figure 18 illustrates the instances of errors of the regression results for the test data set. It is evident that more than 90% of data has a regression error within the range [-0.003 +0.003], which is negligible compared with the target damage severities, indicating a high quality of regression. Figure 19 shows the network outputs with respect to target damage severities for the test data sets. It is evident that the fit is reasonably good, with an R-value above 0.99.

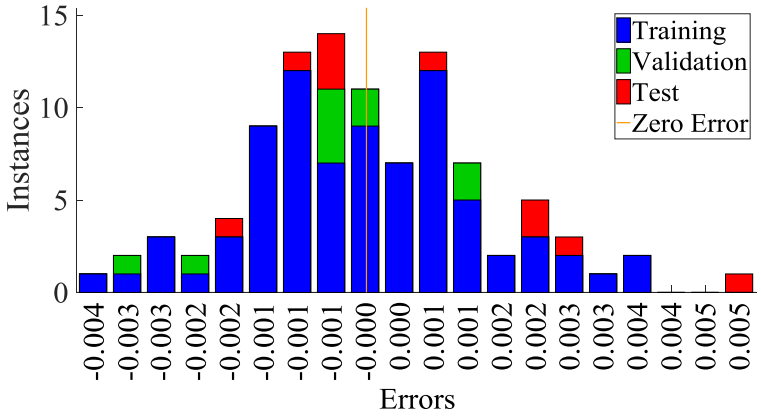

Figure 18
Errors of damage severity regression using neural network (one damage location)

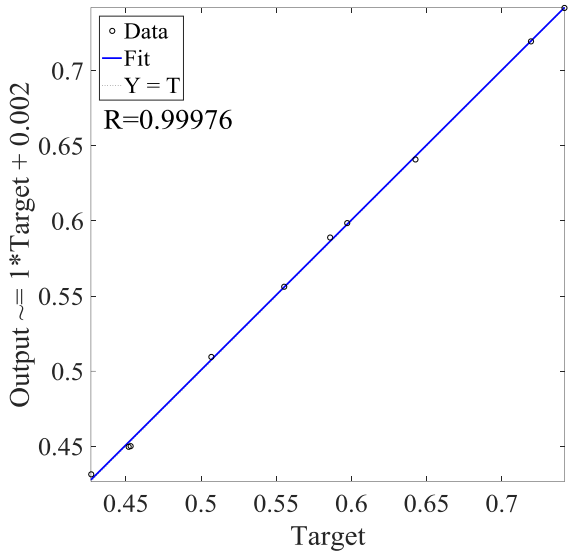

Figure 19
Plots of regressions for the targets and outputs of the test data (one damage location)

Two damage location

Figure 20 and Figure 21 show the results of damage severity regression for the two-damage-location case using the neural networks method. Similar to the one-damage-location cases, most instances have a regression error below 0.01. The plot of regression of the target and output for the test data set has an R of 0.98916. The main reason for the lower quality of damage severity quantification for the two-damage-location cases is that the regression target in this case is a two-element vector indicating the damage severity at each of the damage locations.

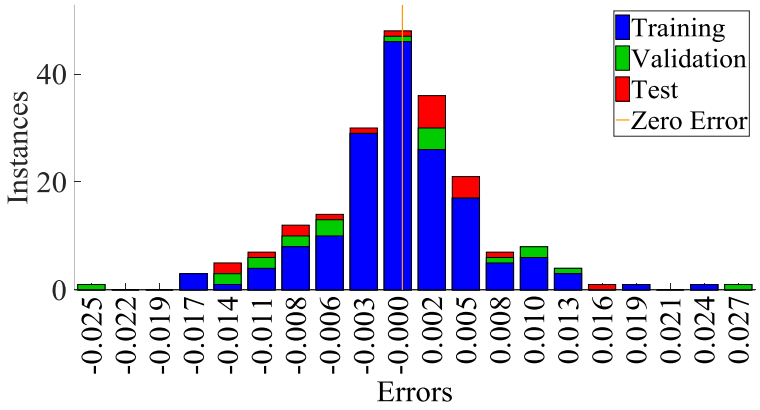

Figure 20
Errors of damage severity regression using neural network (two damage location)

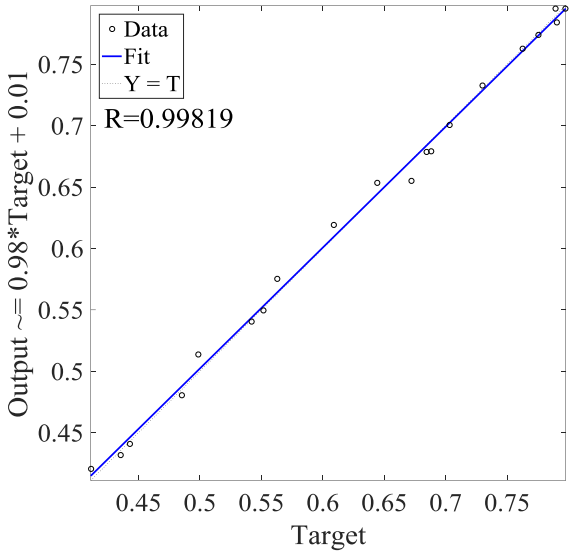

Figure 21
Plots of regressions for the targets and outputs of the test data (two damage location)

Three damage location

Figure 22 and Figure 23show the results of damage severity regression for the three-damage-location case using the neural networks method. Similar to the one-damage-location and two-damage-locations cases, most instances have a regression error below 0.02. The plot of regression of the target and output for the test data set has an R of 0.98317. The main reason for the lower quality of damage severity quantification for the three-damage-location cases is that the regression target in this case is a three-element vector indicating the damage severity at each of the damage locations.

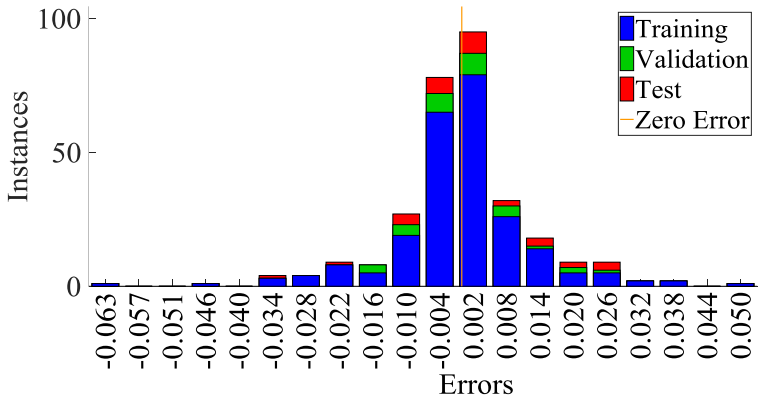

Figure 22
Errors of damage severity regression using neural network (three damage location)

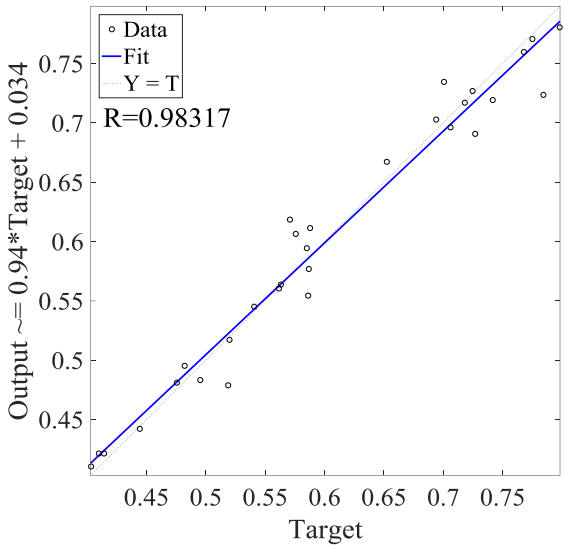

Figure 23
Plots of regressions for the targets and outputs of the test data (three damage location)

Damage diagnosis of a three-span reinforced concrete bridge

On the basis of the damage diagnosis study regarding the 8-DOF structure, bridge damage diagnosis is conducted in this section with respect to the bridge girders, the piers, and the foundation (scour).

Model description

The bridge used in this project is a concrete rigid frame bridge with a span layout of 103 + 180 +103 m, see Figure 24. Figure 25 delineates the damage introduction and sensor installation on the bridge girders. This numerical study quantifies the damage using the reduction of material modulus of elasticity by a certain ratio. Damage can happen at the girder-column joints and the span centers. For simplicity, this numerical simulation introduces only damage weakening the bending stiffness in the elevation plane. The sensors installed at the joints and the locations of multiples of quarter spans can detection the variation of vertical position and rotation in the elevation plane, when the bridge is under dynamic loading. Figure 26 shows the impact loading at the quarter mid-span on the bridge girder. As shown in Figure 27, a Finite Element (FE) model was created using ANSYS. Beam 4 element was used in the model.

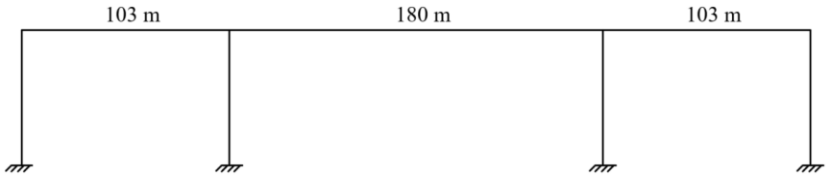

Figure 24
The layout of the rigid frame bridge model

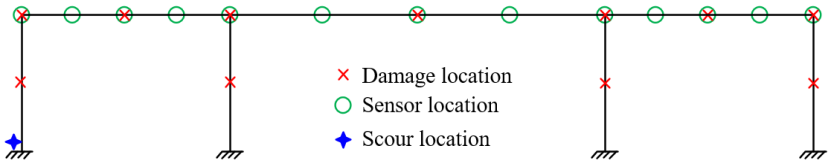

Figure 25
Damage introduction and sensor placement (sensor locations are numbered from 1 to 13 from left to right)

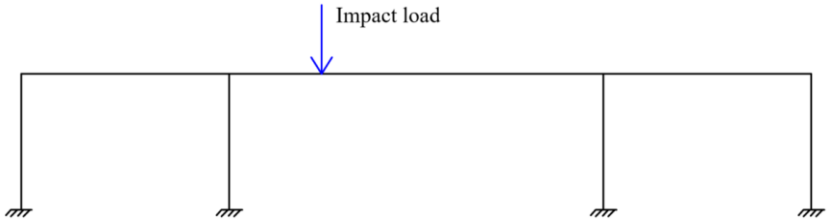

Figure 26
Impact load applied at a quarter position of the mid-span on the bridge

Figure 27
The finite element model of bridge

Dynamic response

Dynamic response and the extracted features from the response corresponding to a two damage case (damage @ location 3 and 6) are illustrated here as a representative. Figure 28Figure 28

Mid-span displacement time history in undamaged and damaged conditions shows the mid-span displacement under impact load under the undamaged and damaged conditions. Figure 29 and Figure 30 show the decomposed modal response under undamaged and damaged conditions. Figure 31 and Figure 32 show the response spectrum under undamaged and damaged conditions. Figure 33 shows the comparison of normalized mode shape between the undamaged and damaged case. Figure 34 shows the comparison of the modal curvature between the undamaged and damaged case. Table 7 lists the modal frequencies of the undamaged and damaged structure. One can find in Figure 33, Figure 34 and Table 7 that two damage locations @ 3 and 6 can cause significant variations of the natural frequency the mode shapes and the modal curvature.

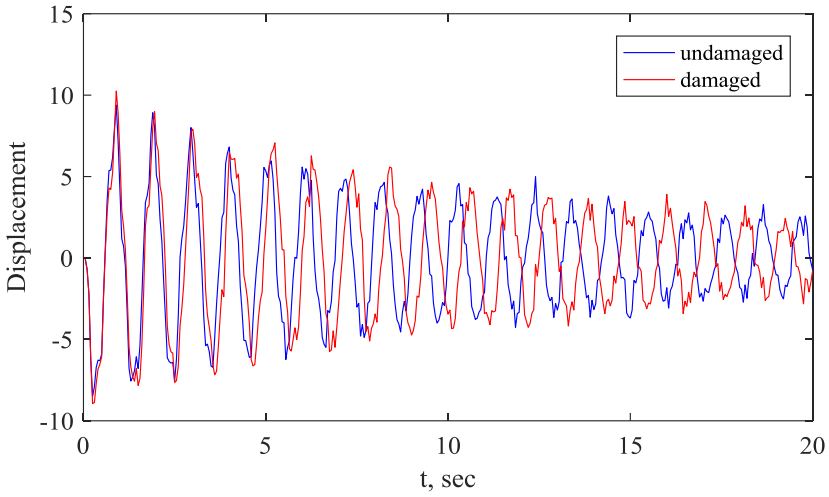

Figure 28
Mid-span displacement time history in undamaged and damaged conditions

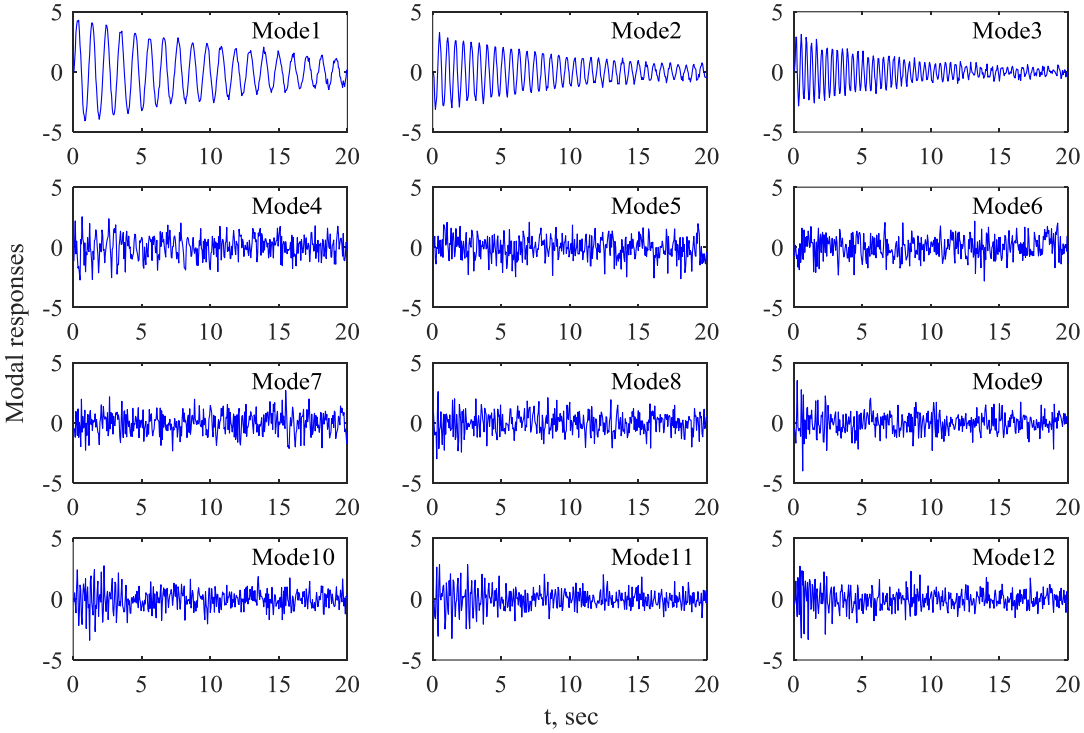

Figure 29
Bridge modal responses in undamaged conditions

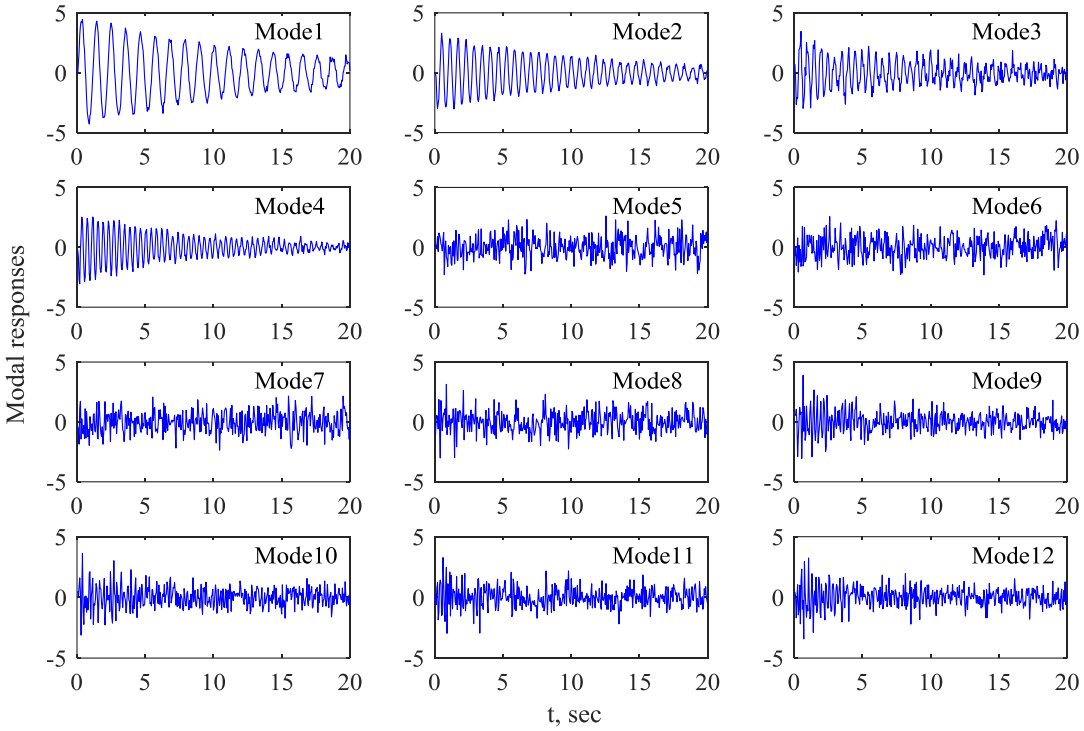

Figure 30
Bridge modal responses under impact load in damaged conditions

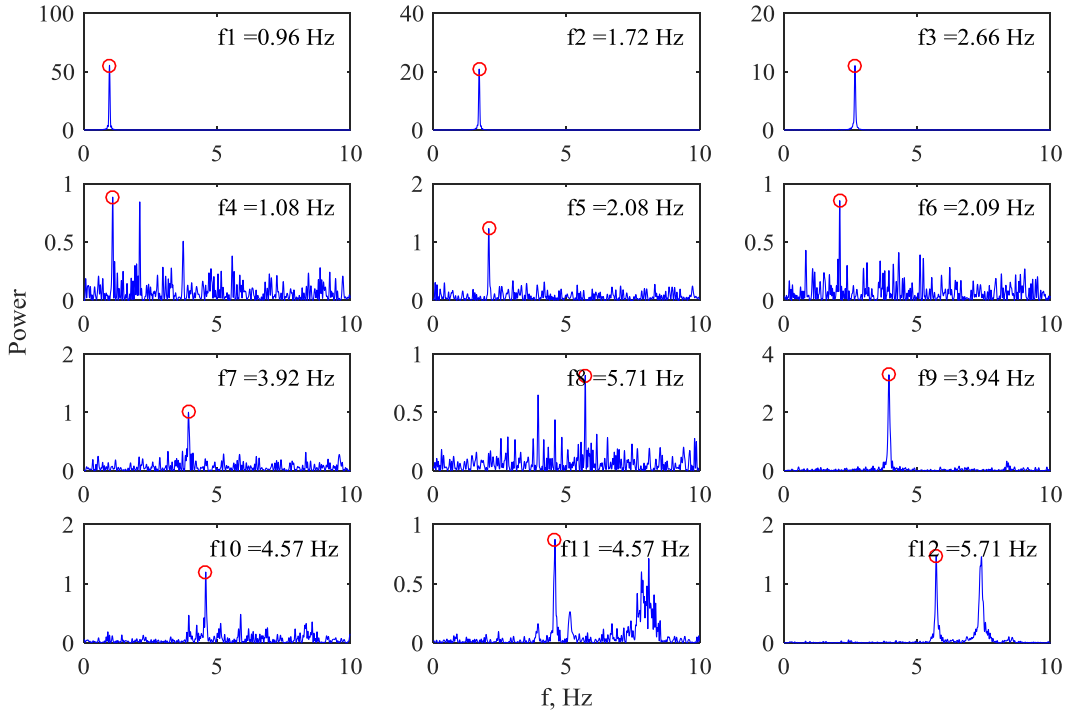

Figure 31
Bridge modal response spectra under impact load in undamaged condition

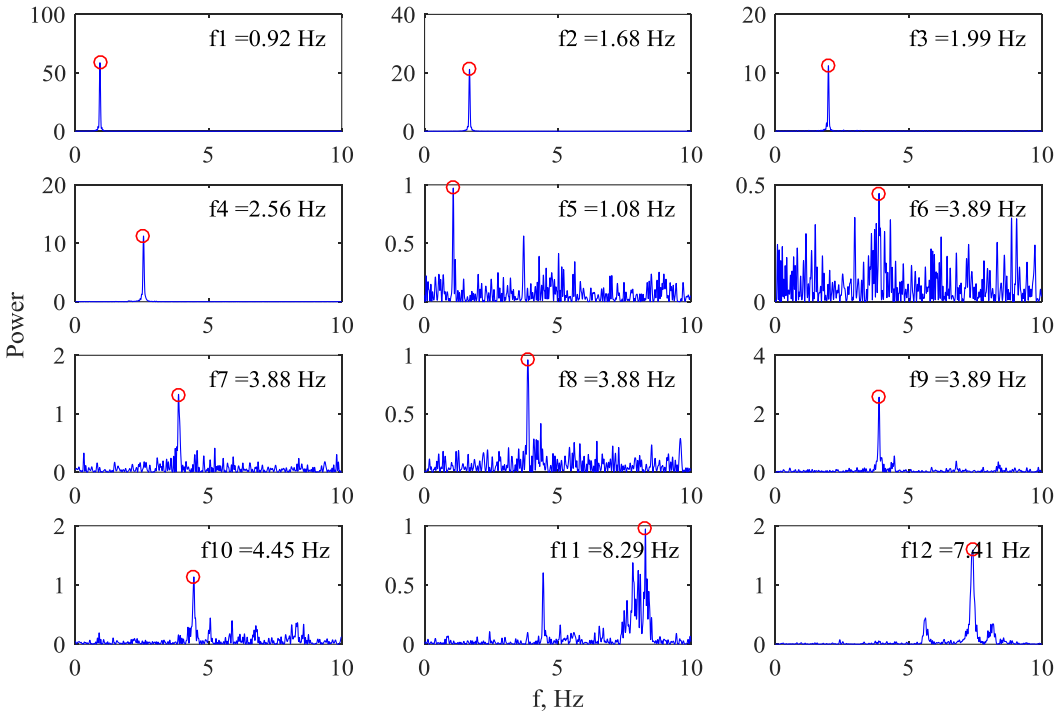

Figure 32
Bridge modal response spectra under impact load with two damage locations

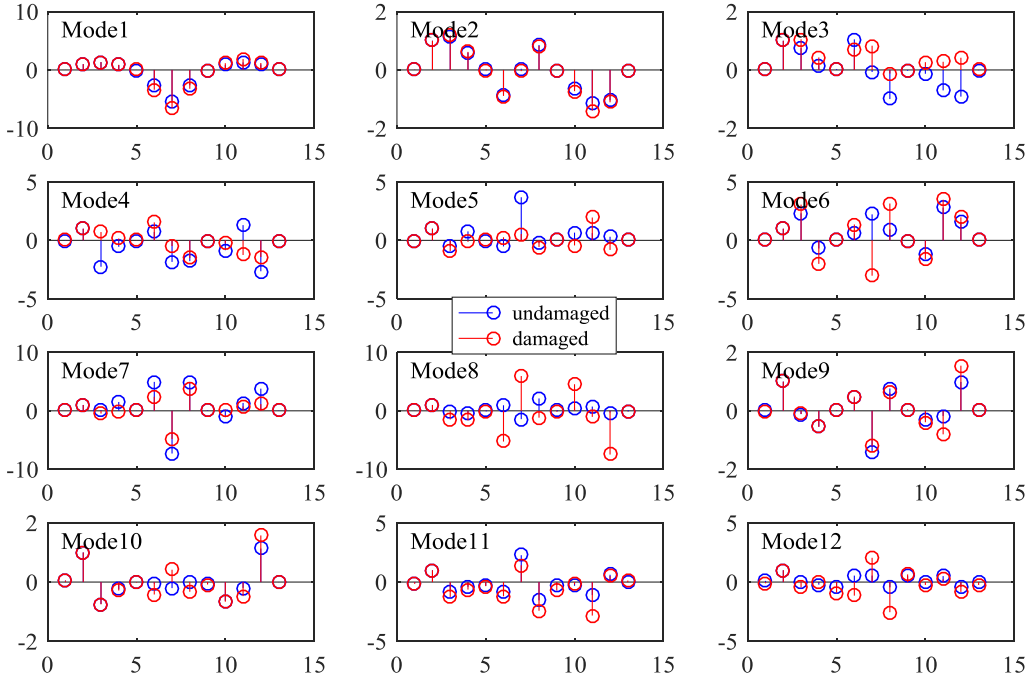

Figure 33
Normalized mode shape comparison between undamaged and damaged conditions

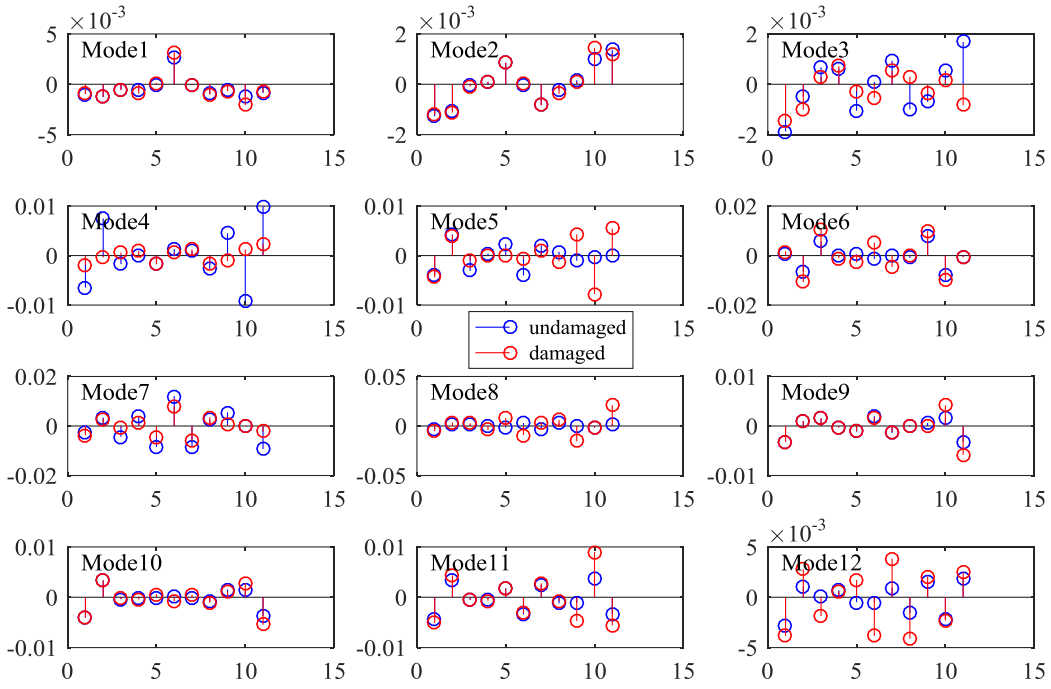

Figure 34
Modal curvature comparison between undamaged and damaged conditions

Table 7
Extracted frequencies of the undamaged and damaged bridge (Unit: Hz)

Mode ID	1	2	3	4	5	6	7	8	9	10	11	12
undamaged	1.0	1.7	2.7	1.1	2.1	2.1	3.9	5.7	3.9	4.6	4.6	5.7
damaged	0.9	1.7	2.0	2.6	1.1	3.9	3.9	3.9	3.9	4.4	8.3	7.4

Girder damage detection and localization

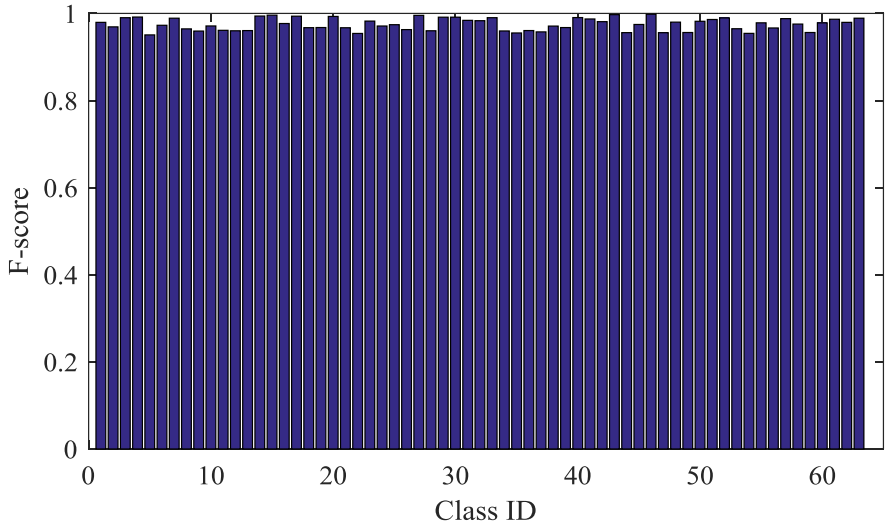

Figure 35
F-score of multi-class classification using 100 data points

Figure 35 lists the f-scores of multi-class classification for damage detection. A total number of 63 cases including 7 cases for single damage location, 21 for two damage location, and 35 for three damage location. It is found in Figure 35 that the f-scores are above 0.95 for all the classes, indicating a high quality of damage detection and localization for the bridge structure.

Girder Damage quantification

One damage location

Figure 36 and Figure 37 show the results of damage severity regression for the one-damage-location cases using neural networks. Figure 36 illustrates the instances of errors of the regression results for the test data set. It is evident that more than 90% of data has a regression error within the range [-0.03 +0.03], which is negligible compared with the target damage severities, indicating a high quality of regression. Figure 37 shows the network outputs with respect to target damage severities for the test data sets. It is evident that the fit is reasonably good, with an R above 0.99.

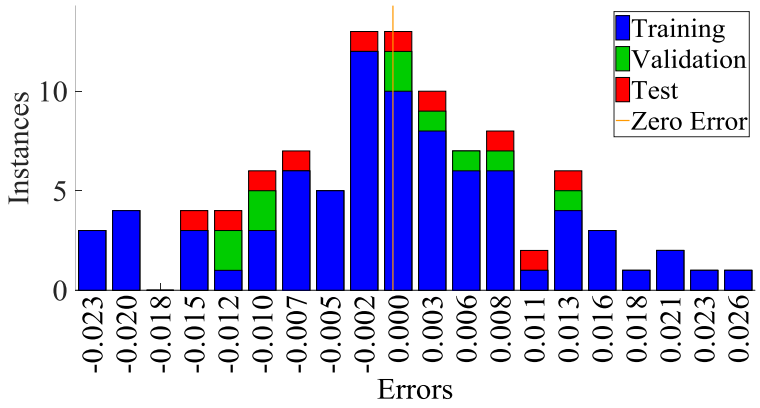

Figure 36
Errors of damage severity regression using neural network (one damage location)

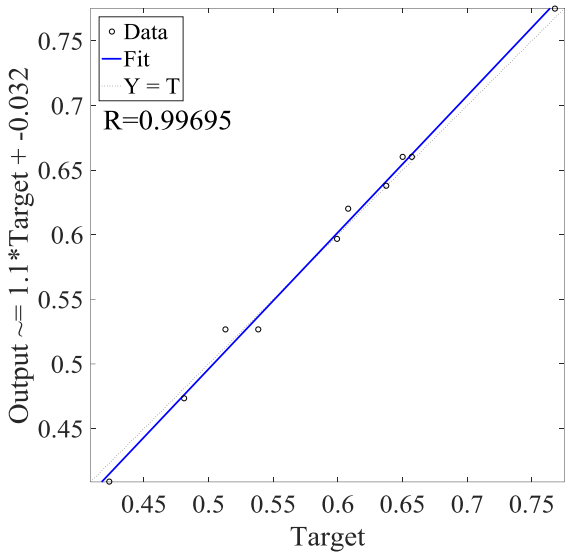

Figure 37
Plots of regressions for the targets and outputs of the test data (one damage location)

Two damage locations

Figure 38 and Figure 39 show the results of damage severity regression for the two-damage-location cases using neural networks. Similar to the one-damage-location cases, most instances have a regression error below 0.05. The plot of regression of the target and output for the test data set has an R of 0.98916. The main reason for the lower quality of damage severity quantification for the two-damage-location cases is that the regression target in this case is a two-element vector indicating the damage severity at each of the damage locations.

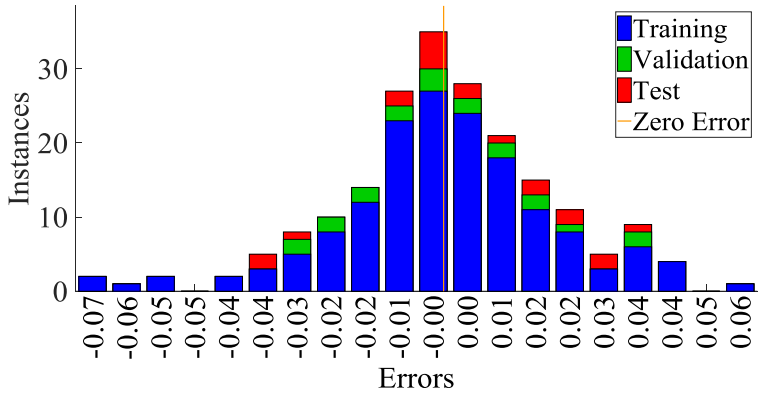

Figure 38
Errors of damage severity regression using neural network (two damage location)

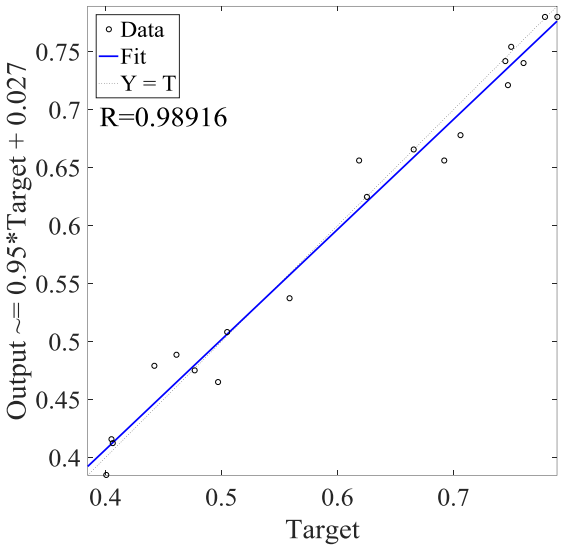

Figure 39
Plots of regressions for the targets and outputs of the test data (two damage location)

Three damage locations

Figure 40 and Figure 41 show the results of damage severity regression for the three-damage-location cases using neural networks. Similar to the one-damage-location cases, most instances have a regression error below 0.05. The plot of regression of the target and output for the test data set has an R of 0.93279. The main reason for the lower quality of damage severity quantification for the three-damage-location cases is that the regression target in this case is a three-element vector indicating the damage severity at each of the damage locations.

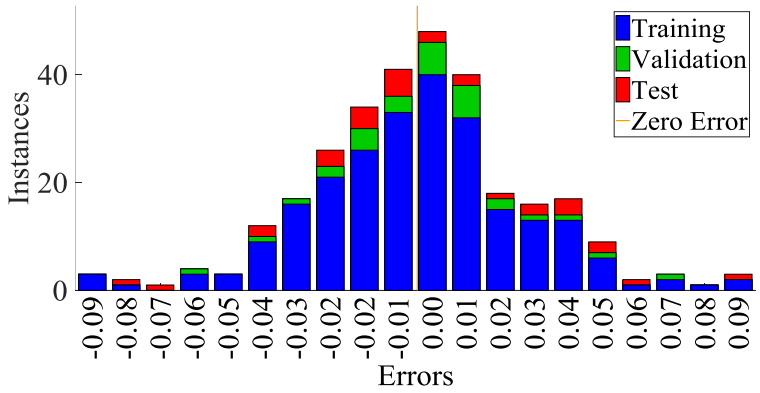

Figure 40
Errors of damage severity regression using neural network (three damage location).

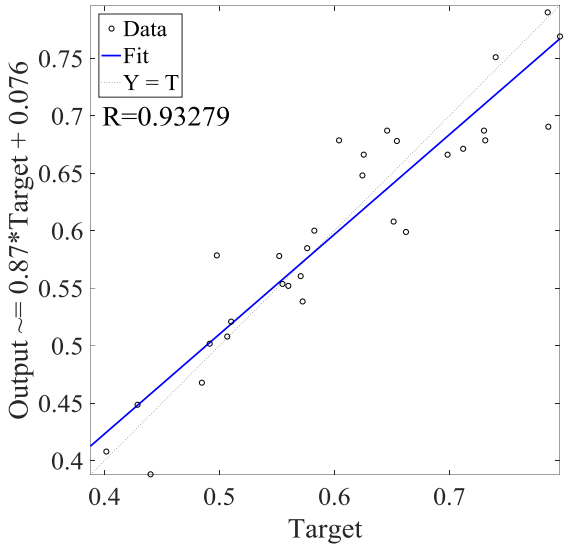

Figure 41
Plots of regressions for the targets and outputs of the test data (three damage location).

Pier damage detection and location

This section presents the results of damage localization and quantification of the bridge piers. It is assumed that there can be at most two piers damaged and the damage always happen at the center of the piers. It is worth noting that the pier damage detection and quantification uses the bridge modal information extracted from the girder responses.

Figure 42 lists the f-scores of the ten categories for damage detection, i.e., four for one-damage-location cases and six for two-damage-location cases. Compared with the girder damage detection results, the pier damage detection has low f-scores with all of them below 0.95 of 90% of them below 0.90. The main reason is that the stiffness reduction on a certain pier may not lead to significant alteration of the girder modal properties, especially considering the fact that there are four piers supporting the bridge girder and that this analysis extracts only a limited number of modes from the girder responses.

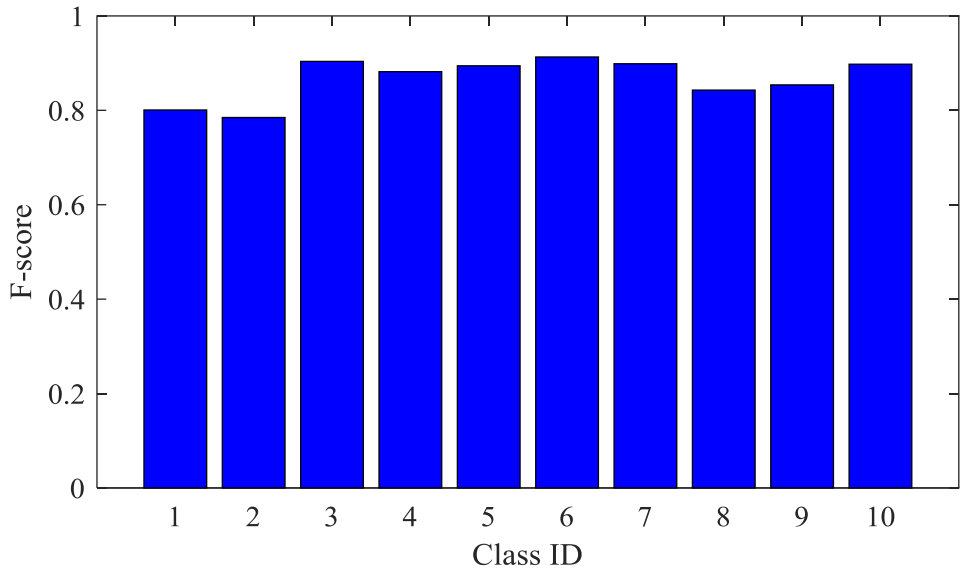

Figure 42
F-score of multi-class classification using data of 100 repeats

Damage severity quantification

The damage severity quantification assumes that the damage location has been located via classification and estimates the damage ratio using the neural network regression module.
Figure 43
Errors of damage severity regression of bridge pier (one damage location)

One damage location

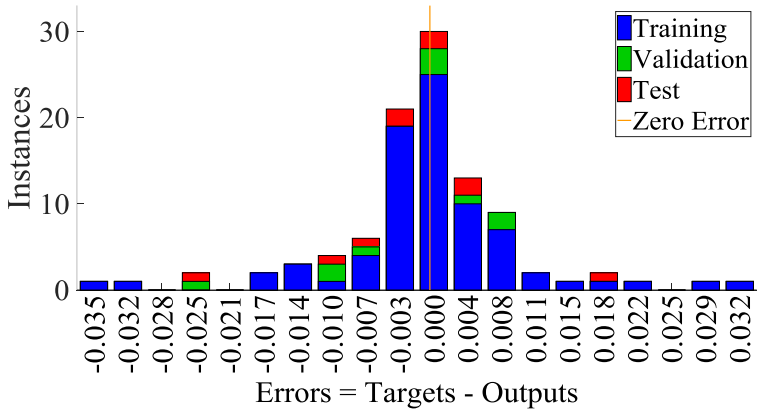

Figure 43
Errors of damage severity regression of bridge pier (one damage location)

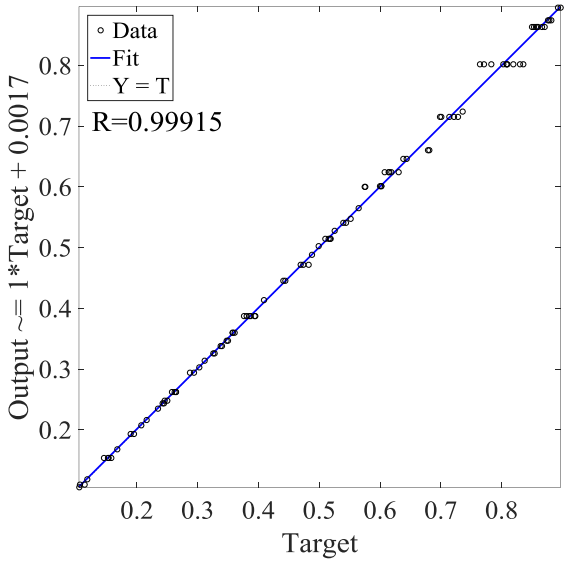

Figure 44
Plots of regressions for the targets and outputs of the test data (one damage location)

Two damage locations

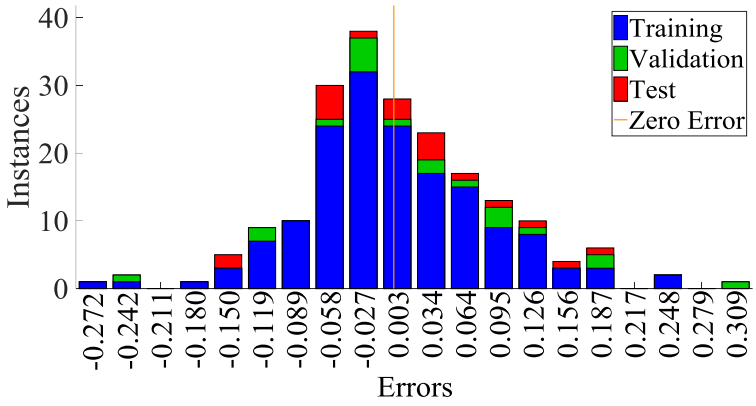

Figure 45
Errors of damage severity regression (two damage location)

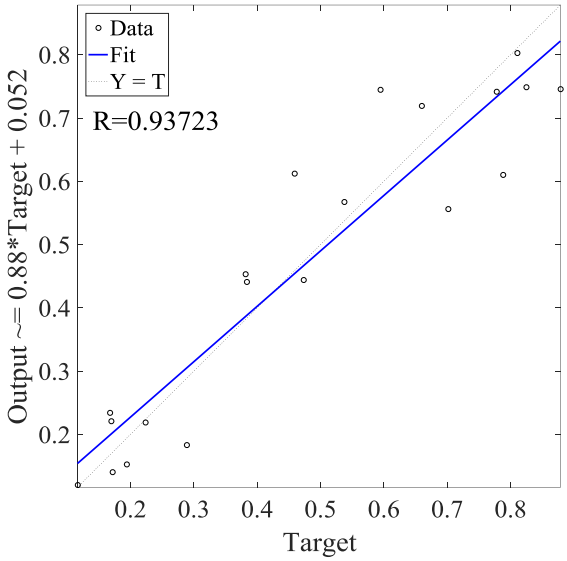

Figure 46
Plots of regressions for the targets and outputs of the test data (one damage location)

Scour damage quantification

Scour issues are the most important factor that causes bridges to collapse. More than 1000 bridges in the United States have collapsed over the past 30 years, with 60% of the failures caused by scouring. With an increasing rate of floods and storm in Louisiana coastal area, the bridges are suffering from more and more severe scouring conditions.

Structurally, scour could cause constraint release on the bridge foundations, which has the potential to lead to bridge modal property alteration. As a preliminary study, this section evaluates the scour severity that is represented by the constraining strength reduction through bridge modal property analysis. This analysis assumes that the scour happens on the left bridge pier as depicted in Figure 25.

Dynamic response of the bridge with scour

Dynamic responses and the extracted features of the pier where the scour occurs are illustrated. Figure 47 shows the pier displacement under the impact load with and without scour. Figure 48 and Figure 49 show the decomposed modal response with and without scour. Figure 50 and Figure 51 show the response spectrum with and without scour. Figure 52 shows the comparison of normalized mode shape. Figure 53 shows the comparison of the modal curvature between the cases with and without scour. One can find in Figure 52 and Figure 53 that the scour in the mid pier can cause significant variations of the natural frequency the mode shapes and the modal curvature.

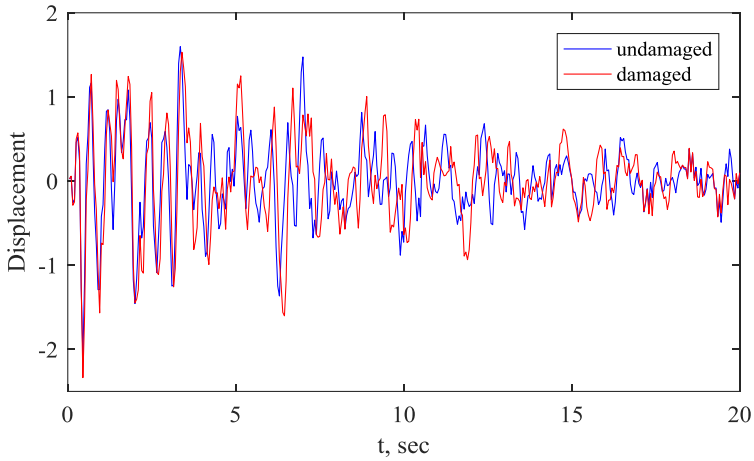

Figure 47
Mid-pier displacement time history with and without scour

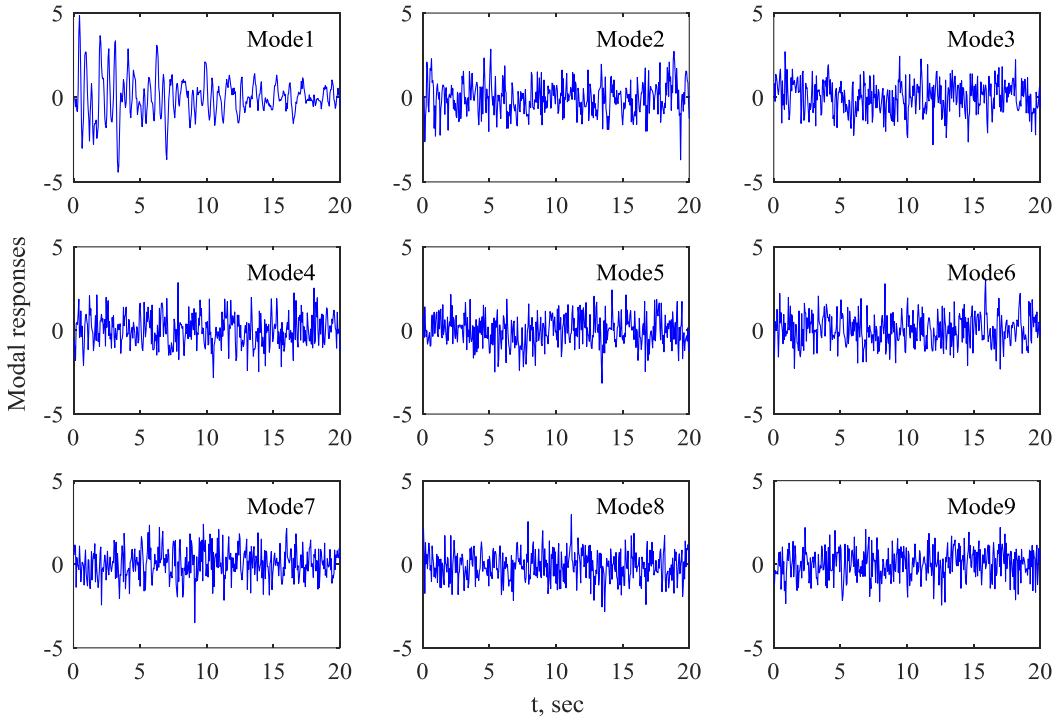

Figure 48
Modal responses without scour

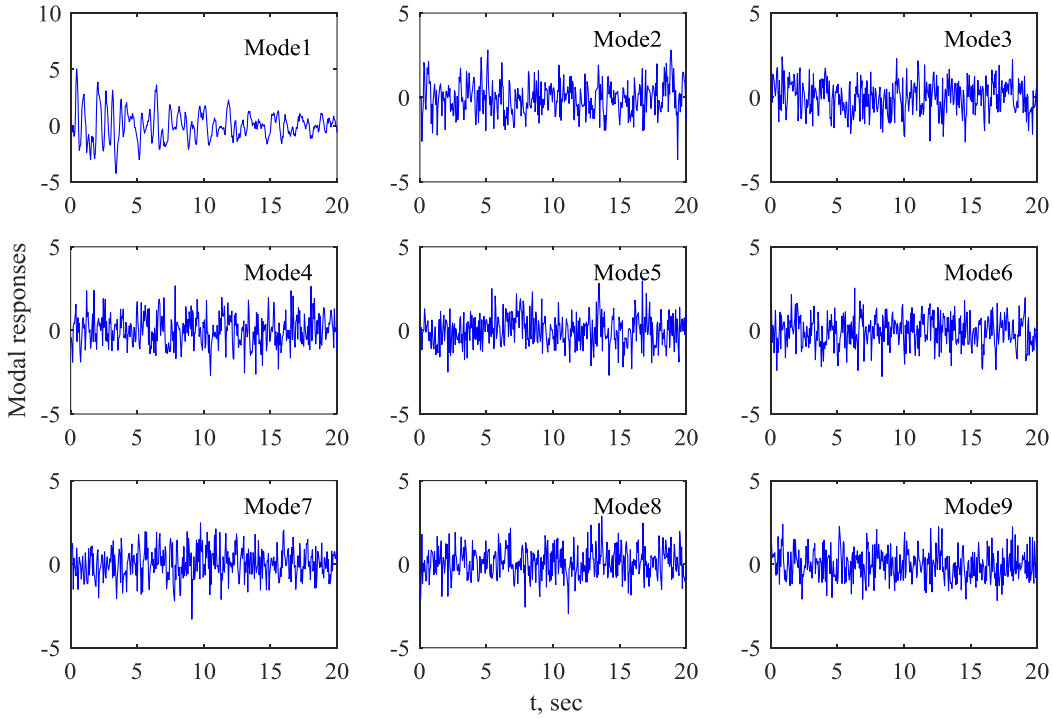

Figure 49
Modal responses with scour

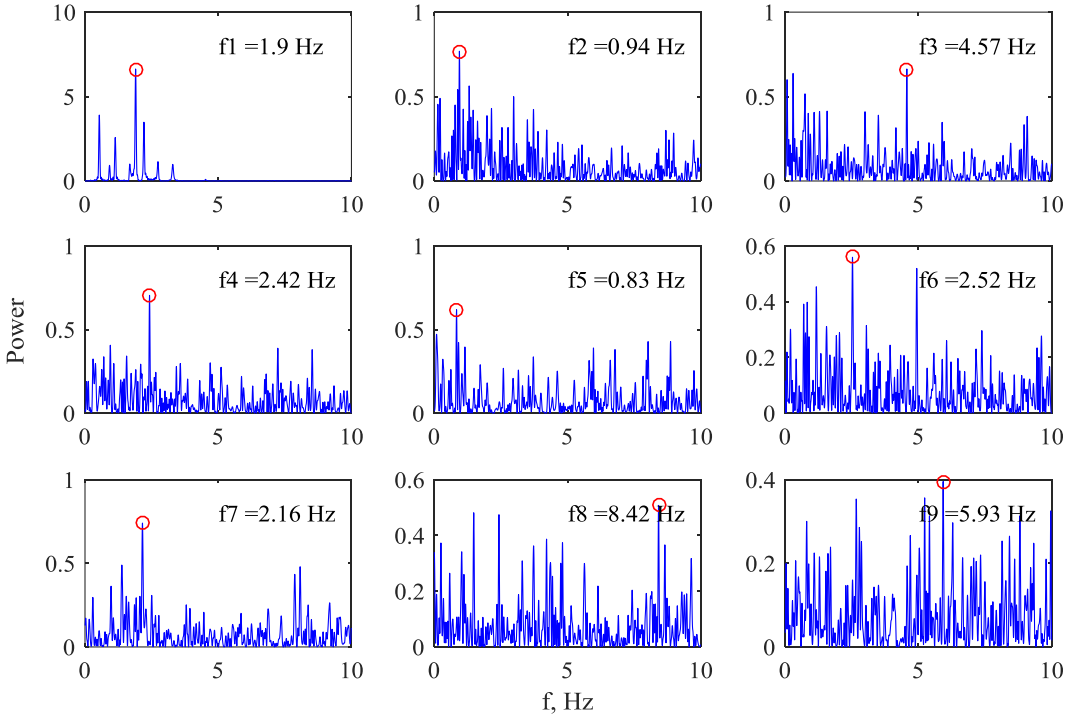

Figure 50
Modal response spectra without scour

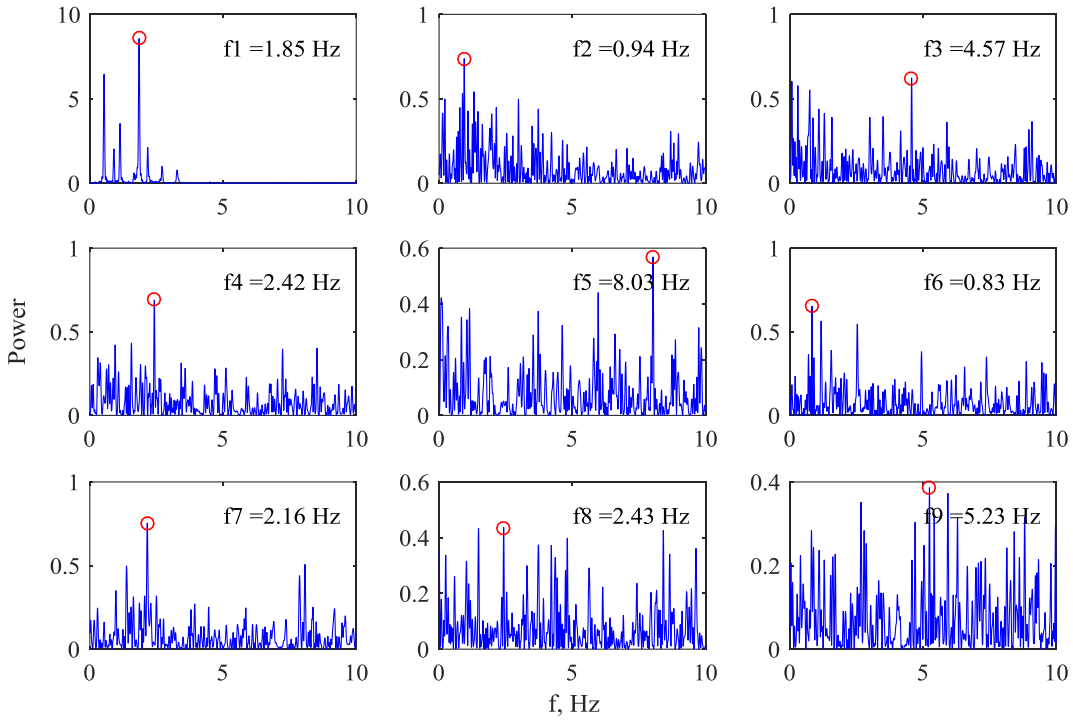

Figure 51
Modal response spectra without scour

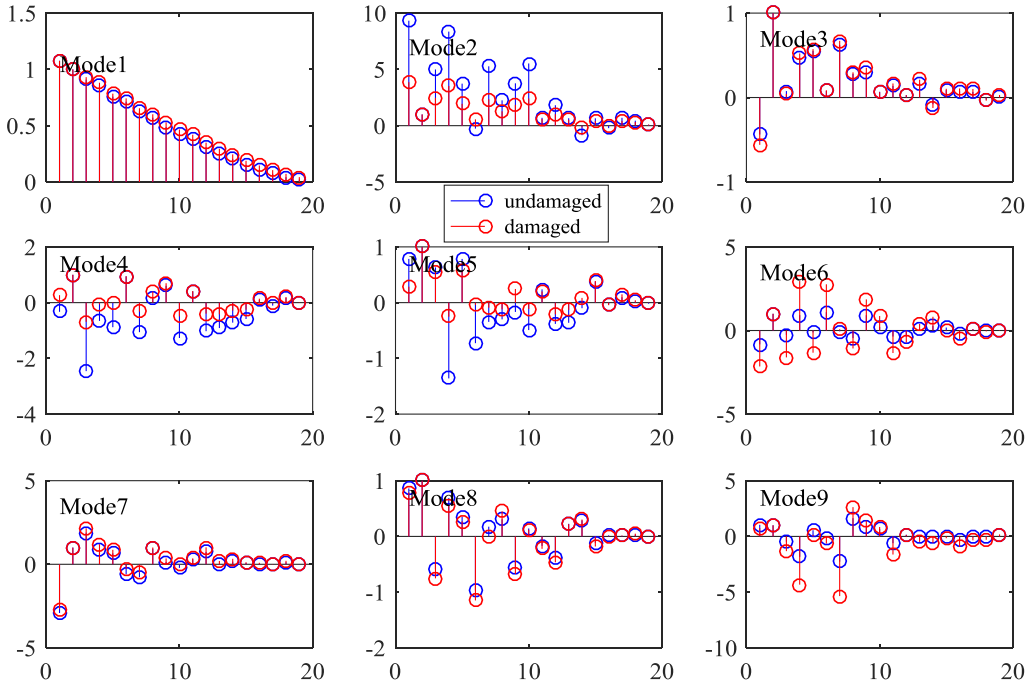

Figure 52
Modal shape comparison between with and without scour

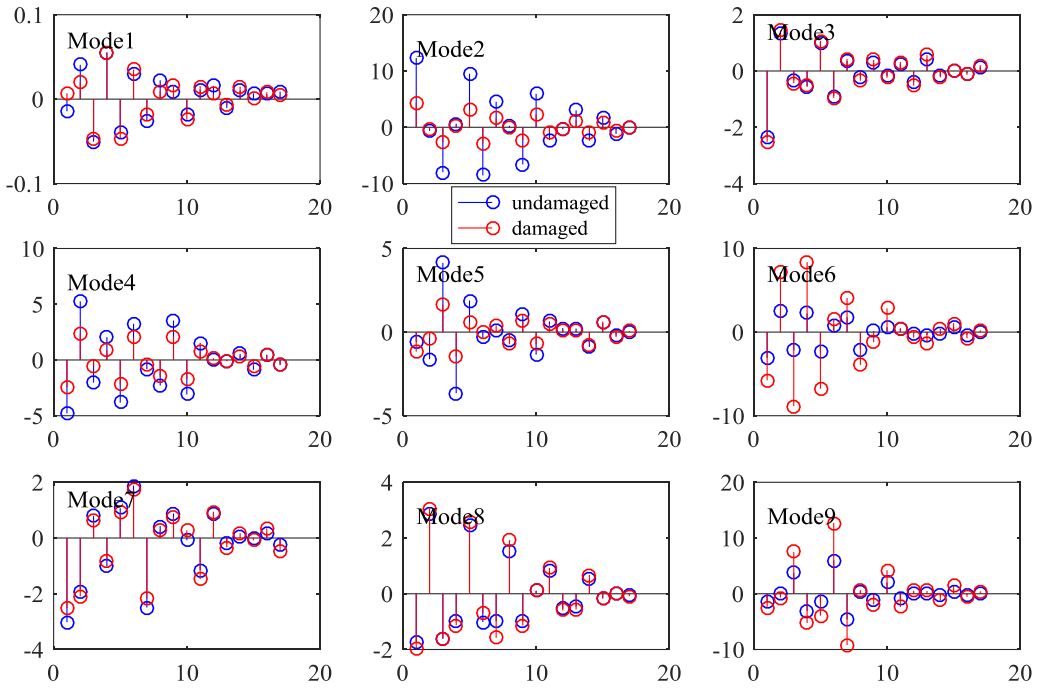

Figure 53
Modal curvature comparison between with and without scour

Scour damage quantification

Figure 54 and Figure 55 show the results of scour damage severity quantification using neural network regression. It is indicated that a high regression quality with low magnitudes of errors and a high R-value are achieved, signaling that the scour severity can be quantified reasonably well using the established NNs method.

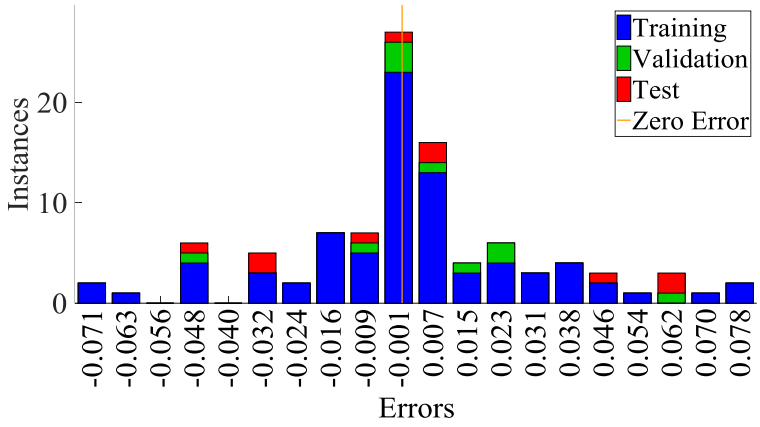

Figure 54
Errors of damage severity regression using neural network

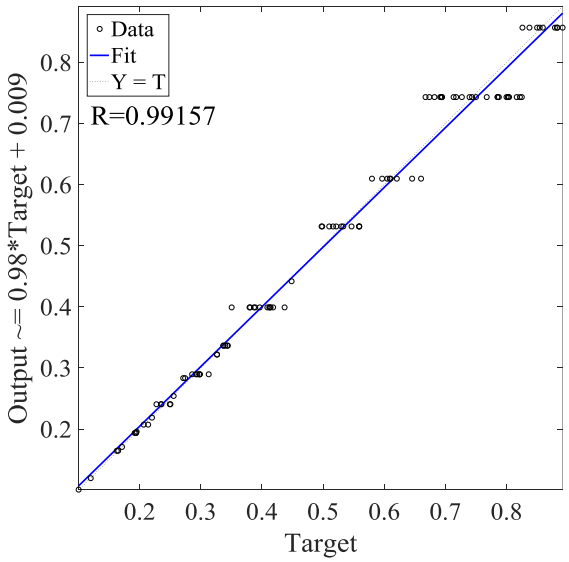

Figure 55
Plots of regressions for the targets and outputs of the test data

CONCLUSIONS

A data-driven framework for coastal bridge damage diagnosis has been established and evaluated numerically. Pattern recognition through supervised machine learning methods is used for damage diagnosis. To reduce the computational cost, damage localization and quantification are implemented in two steps: the first step detects and localizes the damage presence using the classification approach and the second step quantifies the damage using the classification or the regression approach (both are tried in the project). It is indicated that this two-step strategy can efficiently and accurately detect and quantify the damage.

Normalized modal frequency variation, mode shape variation and modal curvatures are extracted and utilized as damage indicative features. It is demonstrated that these extracted features can satisfactorily represent the damage presence.

On the basis of the preliminary study with respect to the 8-DOF generalized system, the multi-layer neural networks (NNs) method is shown efficient and accurate and thus selected for the framework. Among the multi-class classification, the binary classification and the multi-label classification approaches, the multi-label classification approach is proved to be the most efficient. In the case of the 8-DOF system, with 100 data points, the F-score of multi-label classification is around 0.95 while the multi-class classification approach needs around 1000 data points to produce a comparable F-score value. In the case of binary classification, the F-score with 1000 data points is around 0.95 for “no damage” while the F-score is lower than 0.8 for many “damage” cases.

When the established framework was applied for damage diagnosis of the 3-span reinforced concrete bridge, the damage presence in the bridge girders and the piers can be detected and quantified well. For damage detection and localization, the F-score is above 0.95 with 100 data points for each case. For damage quantification, the regression of the output and the target has a high R value around 0.98. In addition, the bridge scour can also be quantified well.

To sum, the established framework is promising for damage diagnosis of bridges and also a wide range of structural and mechanical structures using a data-driven approach. Since the implemented research in this project is exploratory and numerical, further experimental study will be performed to verify the established framework.

RECOMMENDATIONS

Damage diagnosis (localization and quantification) is the first step to develop a decision making framework for bridge operation management. The final target for bridge condition assessment is to implement damage prognosis which predicts the remaining useful life of bridges under the current health state (done by damage diagnosis) and a probabilistic future loading model. Therefore, based on the results presented in this project, recommendations stemming out of this research are summarized as follows:

(1) A data-driven system for damage diagnosis is used for real bridges, especially those old bridges that are probably damaged.

(2) A full research project needs to be conducted to verify the established framework using experimental and filed test data.

(3) Another full research project needs to be conducted to develop a complete data-driven framework for decision-making of bridge management which is capable to include climate data (hurricane, storm surges, waves and floods), traffic data and other relevant data.

(4) A pilot study is recommended to use unmanned aerial vehicle for data acquisition from real bridges to apply the established framework.

ACRONYMS, ABBREVIATIONS, & SYMBOLS

LTRC	Louisiana Transportation Research Center
ANN	Artificial Neural Networks
DOF	Degree of Freedom
DSI	Damage Signature Index
FE	Finite Element
FFC	Fractional Frequency Change
InsDif	Instance Differentiation
LM	Loading Mass
LR	logistic regression
NFCR	Normalized Frequency Change Ratio
SVM	Support Vector Machine
TM	Transmissibility Mass
m	Lumped mass of the system
H	Harmonic excitation
I	Impact load
W	White noise excitation
k	Stiffness coefficient of the spring
c	Damping coefficient of the spring
f	Modal frequency
Φ	Mode shape
v	Modal vector amplitude
h	Distance between two successive measurement locations
v''	Modal curvature
T	Transmissibility function
K	Stiffness Matrix
ω	Circular frequency
M	Mass Matrix

REFERENCES

1. Charles R. Farrar, Nick A. J. Lieven. “Damage Prognosis: the future of structural health monitoring,” Philosophical Transactions, Vol. 365, 2007, pp. 623-632.

2. Teughels A, De Roeck G. “Structural damage identification of the highway bridge Z24 by FE model updating,” Journal of Sound and Vibration, Vol. 278, No. 3, 2004, pp. 589- 610.

3. Moaveni B, Conte JP, Hemez FM. “Uncertainty and Sensitivity Analysis of Damage Identification Results Obtained Using Finite Element Model Updating,” Computer-Aided Civil and Infrastructure Engineering, Vol. 24 No. 5, 2009, pp. 320-34.

4. Friswell MI, “Damage identification using inverse methods,” In: Morassi A, Vestroni F, eds. Dynamic Methods for Damage Detection (CISM Courses and Lectures vol 499). New York, Springer Wien, 2008, pp. 13-66.

5. Worden K, Friswell MI. “Modal vibration-based damage identification,” In: Boller C, Chang F-K, Fujino Y, eds. Encyclopedia of Structural Health Monitoring: John Wiley and Sons, 2009.

6. Doebling, S., Farrar, C., Prime, M. and Shevitz, D. (1996) “Damage Identification and Health Monitoring of Structural and Mechanical Systems from Changes in Their Vibration Characteristics: A Literature Review,” Los Alamos National Laboratory Report LA-13070-MS, available online from Los Alamos National Laboratory, http://library.lanl.gov/.

7. R. J. Allemang and D. L. Brown. “A correlation coefficient for modal vector analysis,” Proceedings of the 1st International Modal Analysis Conference I, 1982, pp. 110–116.

8. V. G. Idichandy and C. Ganapathy. “Modal parameters for structural integrity monitoring of fixed offshore platforms,” Experimental Mechanics, 1990, pp. 382–39.

9. H. J. Salane and J. W. Baldwin. “Changes in modal parameters of a bridge during fatigue testing,” Experimental Mechanics, 1990, pp. 109–113.

10. T. Wolff and M. Richardson. “Fault detection in structures from changes in their modal parameters,” Proceedings of the 7th International Modal Analysis Conference, 1989, pp. 87–94.

11. K. Wyckaert, R. Snoeys and P. Sas. “A feasibility study for the application of frequency monitoring techniques in quality control,” Proceedings of the 5th International Modal Analysis Conference II, 1988, pp. 921–927.

12. W. M. West. “Illustration of the use of modal assurance criterion to detect structural changes in an orbiter test specimen,” Proceedings of the 4th International Modal Analysis Conference I, 1986, pp. 1–5.

13. N. A. J. Lieven and D. J. Ewins. “Spatial correlation of mode shapes, the coordinate modal assurance criterion (comac),” Proceedings of the 5th International Modal Analysis Conference I, 1988, pp. 690–695.

14. M. Biswas, A. K. Pandey and M. M. Samman. “Diagnostic experimental spectral/modal analysis of a highway bridge,” The International Journal of Analytical and Experimental Modal Analysis, Vol. 5, 1989, pp. 33–42.

15. P. Cawley and R. D. Adams. “The location of defects in structures from measurements of natural frequencies,” Journal of Strain Analysis, Vol. 14, 1979, pp. 49–57.

16. Kaminski P C. “The approximate location of damage through the analysis of natural frequencies with artificial neural networks,” J. Process Mech. Eng., Vol. 209, 1995, pp. 117–23.

17. Lam H F, Ko J M and Wong C W. “Localization of damaged structural connections based on experimental modal and sensitivity analysis,” J. Sound Vib. Vol. 210, 1998, pp. 91–115.

18. Chen, Q., et al. “Structural fault detection using neural networks trained on transmissibility functions,” Proceedings of the International Conference on Vibration Engineering, 1994, pp. 567-576.

19. Worden, Keith. “Structural fault detection using a novelty measure,” Journal of Sound and vibration, Vol. 201, No. 1, 1997, 85-101.

20. Worden, Keith, Graeme Manson, and Nick RJ Fieller. “Damage detection using outlier analysis,” Journal of Sound and Vibration, Vol. 229, No. 3, 2000, 647-667.

21. Worden, Keith, Graeme Manson, and David Allman. “Experimental validation of a structural health monitoring methodology: Part I. Novelty detection on a laboratory structure,” Journal of Sound and Vibration, Vol. 259, No. 2, 2003, 323-343.

22. Manson, Graeme, Keith Worden, and David Allman. “Experimental validation of a structural health monitoring methodology: Part II. Novelty detection on a Gnat aircraft,” Journal of Sound and Vibration, Vol. 259, No., 2, 2003, 345-363.

23. Chen, Q. C. Y. W., Y. W. Chan, and K. Worden. ”Structural fault diagnosis and isolation using neural networks based on response-only data,” Computers & Structures, Vol. 81, No. 22, 2003, 2165-2172.

24. Manson, Graeme, Keith Worden, and David Allman. “Experimental validation of a structural health monitoring methodology: Part III. Damage location on an aircraft wing,” Journal of Sound and Vibration, Vol. 259, No. 2, 2003, 365-385.

25. Pandey, A.K., Biswas, M. and Samman, M.M. “Damage detection from changes in curvature mode shapes,” Journal of Sound and Vibration, Vol. 145, 1991, pp. 321–332.

26. Abdel Wahab, M.M. and De Roeck, G. “Damage detection in bridges using modal curvatures: Application to a real damage scenario,” Journal of Sound and Vibration, Vol. 226, 1999, pp. 217–235.

27. Joachims, Thorsten. “Text categorization with support vector machines: Learning with many relevant features,” Machine learning: ECML-98, 1998, pp. 137-142.

28. Yang, Yiming. “An evaluation of statistical approaches to text categorization,” Information retrieval Vol. 1, No.1 1999, pp. 69-90.

29. Schapire, Robert E., and Yoram Singer. “BoosTexter: A boosting-based system for text categorization,” Machine learning, Vol. 39, No. 2, 2000, pp. 135-168.

30. Zhang, M., and Zhi-Hua Zhou. “Multi-label learning by instance differentiation,” Proceedings of the 22nd AAAI Conference on Artificial Intelligence, Vancouver, Canada, 2007, pp. 669–674.

31. Yang, Y. and Nagarajaiah S. “Blind modal identification of output-only structures in time-domain based on complexity pursuit”, Earthquake Engineering & Structural Dynamics, Vol. 42, No. 13, 2013, pp. 1885–1905.

32. Robert E. Schapire，Yoram Singer. “BoosTexter: A Boosting-based System for Text Categorization,” Machine learning, Vol. 39, 2000, pp. 135-168.

APPENDIX

ENGINEERING DRAWINGS OF THE BRIDGE

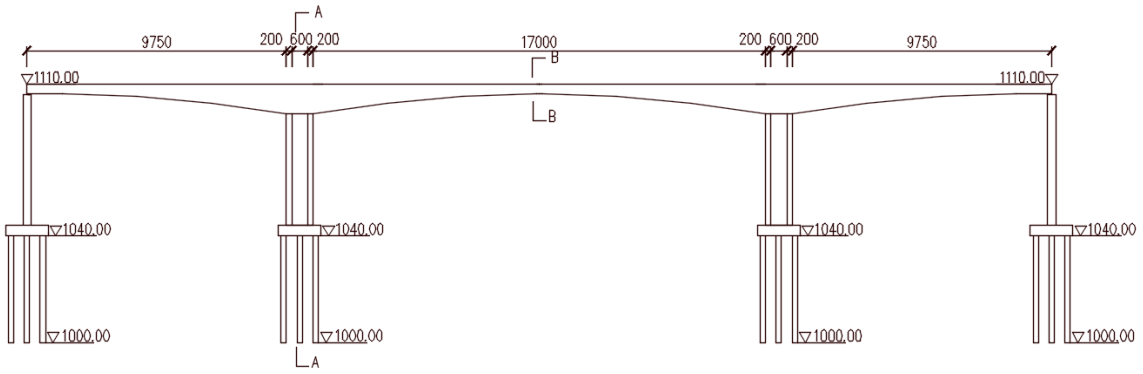

Bridge layout

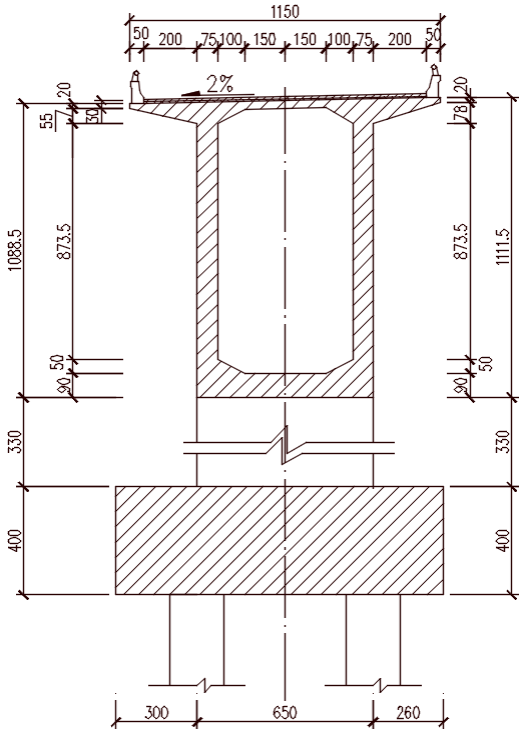

A-A cross section

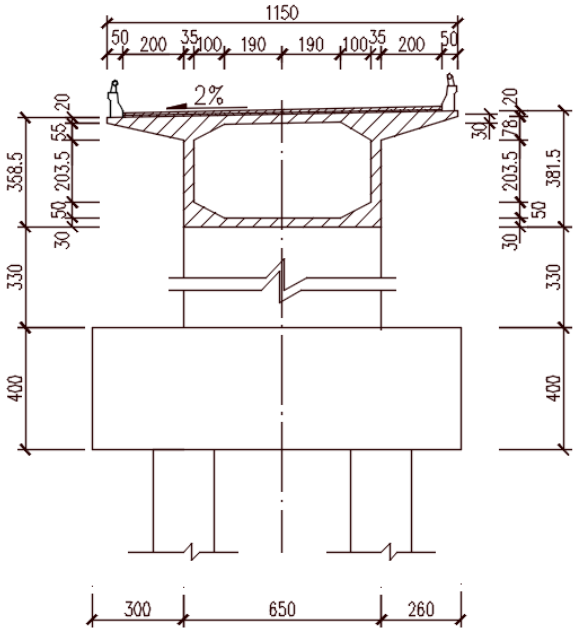

B-B cross section